

The Status of Exotic-quantum-number Mesons

C. A. Meyer¹ and Y. Van Haarlem¹

¹*Carnegie Mellon University, Pittsburgh, PA 15213*

(Dated: May 3, 2010)

The search for mesons with non-quark-antiquark (exotic) quantum numbers has gone on for nearly thirty years. There currently is experimental evidence of three isospin one states, the $\pi_1(1400)$, the $\pi_1(1600)$ and the $\pi_1(2015)$. For all of these states, there are questions about the identification of these state, and even if some of them exist. In this article, we will review both the theoretical work and the experimental evidence associated with these exotic quantum number states. We find that the $\pi_1(1600)$ could be the lightest exotic quantum number hybrid meson, but observations of other members of the nonet would be useful.

PACS numbers: 14.40.-n,14.40.Rt,13.25.-k

I. INTRODUCTION

In the quark model, mesons are bound states of quarks and antiquarks ($q\bar{q}$). The quantum numbers of such fermion-antifermion systems are functions of the total spin, S , of the quark-antiquark system, and the relative orbital angular momentum, L , between them. The parity of such systems is given as $P = -(-1)^L$ and the charge-conjugation quantum number (C-parity) is $C = (-1)^{L+S}$. This leads to mesons having well defined quantum numbers: total angular momentum, J , parity, P , and C-parity, C . These are represented as J^{PC} . For the case of $L = 0$ and $S = 0$, we have $J^{PC} = 0^{-+}$, while for $L = 0$ and $S = 1$, $J^{PC} = 1^{--}$. The allowed quantum numbers for L smaller than three are given in Table I. Interestingly, for J smaller than 3, all allowed J^{PC} except 2^{--} [1] have been observed.

L	S	J^{PC}	L	S	J^{PC}	L	S	J^{PC}
0	0	0^{-+}	1	0	1^{+-}	2	0	2^{-+}
0	1	1^{--}	1	1	0^{++}	2	1	1^{--}
			1	1	1^{++}	2	1	2^{--}
			1	1	2^{++}	2	1	3^{--}

TABLE I. The allowed J^{PC} quantum numbers for $q\bar{q}$ systems.

From the quantum numbers in Table I, there are several combinations which are missing: 0^{--} , 0^{+-} , 1^{+-} and 2^{+-} . These are not possible for simple $q\bar{q}$ systems and are known as “exotic” quantum numbers. Observation of states with exotic quantum numbers has been of great experimental interest as it would be clear evidence for mesons beyond the simple $q\bar{q}$ picture.

Moving beyond the simple quark model picture of mesons, there have been predictions for states with these exotic quantum numbers. The most well known are $q\bar{q}$ states in which the gluons binding the system can contribute directly to the quantum numbers of the meson. However, other candidates include four-quark states ($qq\bar{q}\bar{q}$) and states containing only gluons (glueballs). Early bag-model calculations [2] referred to states with $q\bar{q}$ and gluons as “hermaphrodite mesons”, and predicted that the lightest nonet ($J^{PC} = 1^{-+}$) might have

masses near 1 GeV as well as distinctive decay modes. They might also be relatively stable, and thus observable. While the name hermaphrodite did not survive, what are now known as “hybrid mesons” have become a very interesting theoretical and experimental topic and the status of these states, with particular emphasis on the exotic-quantum number ones is the topic of this article. More information on meson spectroscopy in general can be found in a recent review by Klempt and Zaitsev [3]. Similarly, a recent review on the related topic of glueballs can be found in reference [4].

II. THEORETICAL EXPECTATIONS FOR HYBRID MESONS

A. Notation and Quantum Numbers

The notation used throughout this article to represent hybrid mesons is that which is currently in use by the Particle Data Group (PDG) [1]. In their notation, the parity and charge conjugation determine the name of the hybrid, which is taken as the name of the normal meson of the same J^{PC} and isospin. The total spin is then used as a subscript to the name. While various models predict different nonets of hybrid mesons, the largest number of nonets is from the flux-tube model (see Section IIB). For completeness, we list all of these as well as their PDG names in Table II. The first entry is the isospin one ($I = 1$) state. The second and third are those with isospin equal to zero ($I = 0$) and the fourth is the kaon-like state with isospin one-half ($I = \frac{1}{2}$). In the case of the $I = 0$ states, the first is taken as the state that is mostly $u\bar{u}$ and $d\bar{d}$ (so-called $n\bar{n}$), while the second is mostly $s\bar{s}$. For the $I = 0$ states, C -parity is well defined, but for $I = 1$, only the neutral member can have a defined C -parity. However, the more general G -parity can be used to describe all of the $I = 1$ members. For a state of whose neutral member has C -parity C , and whose total isospin is I , the G -parity is defined to be

$$G = C \cdot (-1)^I,$$

which can be generalized to

$$G = (-1)^{L+S+I}. \quad (1)$$

The latter is valid for all of the $I = 0$ and $I = 1$ members of a nonet. Thus, the G -parity can be used to identify exotic quantum numbers, even for charged $I = 1$ members of a nonet. For the case of the kaon-like states, neither C -parity nor G -parity is defined. Thus, the $I = \frac{1}{2}$ members of a nonet can not have explicitly exotic quantum numbers.

QNs		Names					
J^{PC}	(I^G)	(I^G)	(I)				
1^{++}	(1^-)	a_1	(0^+)	f_1	f'_1	$(\frac{1}{2})$	K_1
1^{--}	(1^+)	ρ_1	(0^-)	ω_1	ϕ_1	$(\frac{1}{2})$	K_1^*
0^{-+}	(1^-)	π_0	(0^+)	η_0	η'_0	$(\frac{1}{2})$	K_0
1^{-+}	(1^-)	π_1	(0^+)	η_1	η'_1	$(\frac{1}{2})$	K_1^*
2^{-+}	(1^-)	π_2	(0^+)	η_2	η'_2	$(\frac{1}{2})$	K_2
0^{+-}	(1^+)	b_0	(0^-)	h_0	h'_0	$(\frac{1}{2})$	K_0^*
1^{+-}	(1^+)	b_1	(0^-)	h_1	h'_1	$(\frac{1}{2})$	K_1
2^{+-}	(1^+)	b_2	(0^-)	h_2	h'_2	$(\frac{1}{2})$	K_2^*

TABLE II. The naming scheme for hybrid mesons. The first state listed for a given quantum number is the isospin one state. The second state is the isospin zero state that is mostly u and d quarks ($n\bar{n}$), while the third name is for the mostly $s\bar{s}$ isospin zero state. Note that for the kaons, the C - and G -parity are not defined. Kaons cannot not have manifestly exotic quantum numbers. States that have exotic quantum numbers are shown in bold.

In Table III we show the J^P of the three exotic $I = 1$ mesons from Table II. We also show the normal ($q\bar{q}$) meson of the same J^P and the I^G quantum numbers for these states. The exotic mesons have the opposite G -parity of the normal meson, which provides a simple mechanism for identifying if a charged $I = 1$ state has exotic quantum numbers.

J^P	normal meson name	(I^G)	exotic meson name	(I^G)
0^+	a_0	(1^-)	b_0	(1^+)
1^-	ρ	(1^+)	π_1	(1^-)
2^+	a_2	(1^-)	b_2	(1^+)

TABLE III. The J^P and I^G quantum numbers for the exotic mesons and the normal mesons of the same J^P .

B. Model Predictions

The first predictions for exotic quantum number mesons came from calculations in the Bag model [5, 6]. In this model, boundary conditions are placed on quarks and gluons confined inside a bag. A hybrid meson is formed by combining a $\bar{q}q$ system (with spin 0 or 1) with a transverse-electric (TE) gluon ($J^{PC} = 1^{+-}$). This

yields four nonets of hybrid mesons with quantum numbers $J^{PC} = 1^{--}, 0^{-+}, 1^{-+}$ and 2^{-+} . These four nonets are roughly degenerate in mass and early calculations predicted the mass of a 1^{-+} to be in the range of 1.2 to 1.4 GeV [7, 8]. In the bag model, the transverse-magnetic gluon is of higher mass. It has $J^{PC} = 1^{-+}$ and combined with the same $S = 0$ and $S = 1$ $\bar{q}q$ systems yield four additional nonets with $J^{PC} = 1^{++}, 0^{+-}, 1^{+-}$ and 2^{+-} . These would presumably be heavier than the nonets built with the TE gluon.

Another method that has been used to predict the hybrid masses are “QCD spectral sum rules” (QSSR). Using QSSR, one examines a two-point correlator of appropriate field operators from QCD and produces a sum rule by equating a dispersion relation for the correlator to an operator product expansion. QSSR calculations initially found a 1^{-+} state near 1 GeV [9, 10]. A 0^{--} state was also predicted around 3.8 GeV in mass [10]. Newer calculations [11] tend to favor a 1^{-+} hybrid mass in the range of 1.6 to 2.1 GeV, and favor the $\pi_1(1600)$ (see Section III C) as the lightest exotic hybrid. Recently, Narison [12] looked at the calculations for $J^{PC} = 1^{-+}$ states with particular emphasis in understanding differences in the results between QSSR and Lattice QCD calculations (see Section II C). He found that the $\pi_1(1400)$ and $\pi_1(1600)$ may be consistent with 4-quark states, while QSSR are consistent with the $\pi_1(2015)$ (see Section III D) being the lightest hybrid meson.

The notion of the formation of flux tubes was first introduced in the 1970’s by Yoichiro Nambu [13, 14] to explain the observed linear Regge trajectories—the linear dependence of mass squared, m^2 , of hadrons on their spin, J . This linear dependence results if one assumes that mass-less quarks are tied to the ends of a relativistic string with constant mass (energy) per length with the system rotating about its center. The linear m^2 versus J dependence only arises when the mass density per length is constant, which is equivalent to a linear potential.

This interpretation, which is known as the “flux-tube model”, has been confirmed in the heavy quark sector using lattice QCD [15]. Within the flux-tube model [16, 17], one can view hybrids as mesons with angular momentum in the flux tube. Naively, one can imagine two degenerate excitations, one with the tube going clockwise and one counter clockwise. It is possible to write linear combinations of these that have definite spin, parity and C -parity. For the case of one unit of angular momentum in the tube, the flux tube behaves as if it has quantum numbers $J^{PC} = 1^{+-}$ or 1^{-+} . The basic quantum numbers of hybrids are obtained by adding the tube’s quantum numbers to that of the underlying meson.

In the flux-tube model, the tube carries angular momentum, m , which then leads to specific predictions for the product of C -parity and parity (CP). For $m = 0$, one has $CP = (-1)^{S+1}$, while for the first excited states, ($m = 1$), we find that $CP = (-1)^S$. The excitations are then built on top of the s -wave mesons, ($L = 0$), where the total spin can be either $S = 0$ or $S = 1$. For the case

of $m = 0$, we find CP as follows,

$$(m = 0) \left. \begin{array}{l} S = 0 \quad 0^{-+} \\ S = 1 \quad 1^{-+} \end{array} \right\} \begin{array}{l} (-1)^{L+1}(-1)^{S+L} = (-1)^{S+1} \\ \text{Normal Mesons} \end{array}$$

which are the quantum numbers of the normal, $q\bar{q}$, mesons as discussed in Section I. For the case of $m = 1$, where we have one unit of angular momentum in the flux tube, we find the following J^{PC} quantum numbers

$$(m = 1) \left. \begin{array}{l} S = 0 \quad 0^{-+} \\ S = 1 \quad 1^{-+} \end{array} \right\} \begin{array}{l} 1^{++}, 1^{--} \\ 0^{-+}, \mathbf{0}^{+-}, \mathbf{1}^{-+}, \mathbf{1}^{+-}, \mathbf{2}^{-+}, \mathbf{2}^{+-} \end{array}.$$

The resulting quantum numbers are obtained by adding both 1^{+-} and 1^{-+} to the underlying $q\bar{q}$ quantum numbers (0^{-+} and 1^{-+}).

From the two $L = 0$ meson nonets, we expect eight hybrid nonets, (72 new mesons!). Two of these nonets arise from the $q\bar{q}$ in an $S = 0$ (singlet) state, while six arise for the $q\bar{q}$ in the $S = 1$ (triplet) state. Of the six states built on the triplet $q\bar{q}$, three have exotic quantum numbers (as indicated in bold above).

In the picture presented by the flux-tube model, the hybrids are no different than other excitations of the $q\bar{q}$ states. In addition to “orbital” and “radial” excitations, we also need to consider “gluonic” excitations. Thus, the flux-tube model predicts eight nonets of hybrid mesons (0^{+-} , 0^{-+} , 1^{++} , 1^{--} , 1^{-+} , 1^{+-} , 2^{-+} and 2^{+-}). The model also predicted that all eight nonets would be degenerate in mass, with masses expected near 1.9 GeV [17].

An alternate approach to calculating properties of hybrid mesons comes from the effective QCD Coulomb-gauge Hamiltonian. Here, Fock states for hadrons are constructed from the vacuum as well as quark and gluon operators. In this model, the lightest hybrid nonets are $J^{PC} = 1^{+-}$, 0^{++} , 1^{++} and 2^{++} , none of which are exotic. The first excitation of these ($L = 1$), yields the nonets 1^{-+} , 3^{-+} and 0^{-+} , all of which are exotic [18]. In this model, the 1^{-+} is the lightest exotic quantum number hybrid, with a mass in the range of 2.1 to 2.3 GeV. Predictions are also made for the lightest $c\bar{c}$ exotic hybrid, which is found in the range of 4.1 to 4.3 GeV.

In Table IV are presented a summary of the mass predictions for the various model calculations for hybrid meson masses.

Mass (GeV)	Model	Reference
1.0-1.4	Bag Model	[2, 5, 6]
1.0-1.9	QSSR	[9–12]
1.8-2.0	Flux Tube	[17]
2.1-2.3	Hamiltonian	[18]

TABLE IV. Mass predictions for hybrid mesons from various models.

C. Lattice Predictions

Lattice QCD (LQCD) calculations may provide the most accurate estimate to the masses of hybrid mesons. While these calculations have progressively gotten better, they are still limited by a number of systematic effects. Currently, the most significant of these is related to the mass of the light quarks used in the calculations. This is typically parametrized as the “pion mass”, and extrapolations need to be made to reach the physical pion mass. This is often made as a linear approximation, which may not be accurate. In addition, as the the quark mass becomes lighter, two-meson decay channels become possible. These may distort the resulting spectrum.

Most calculations have been performed with what is effectively the strange-quark mass. However, it may not be safe to assume that this is the mass of the $s\bar{s}$ member of the nonet, and one needs to be aware of the approximations made to move the estimate to the $u\bar{u}/d\bar{d}$ mass. The bottom line is that no one would be surprised if the true hybrid masses differed by several hundred MeV from the best predictions.

Author Collab.	1^{-+} Mass (GeV/ c^2)	
	$u\bar{u}/d\bar{d}$	$s\bar{s}$
UKQCD [19]	1.87 ± 0.20	2.0 ± 0.2
MILC [20]	$1.97 \pm 0.09 \pm 0.30$	$2.170 \pm 0.080 \pm 0.30$
SESAM [21]	1.9 ± 0.20	
MILC [22]	$2.11 \pm 0.10 \pm (sys)$	
Mei [23]	$2.013 \pm 0.026 \pm 0.071$	
Bernard [24]	1.792 ± 0.139	2.100 ± 0.120
Hedditch [25]	1.74 ± 0.25	
McNeile [26]	2.09 ± 0.1	

TABLE V. Recent results for the light-quark 1^{-+} hybrid meson masses.

While the flux-tube model (see Section II B) predicts that the lightest eight nonets of hybrid mesons are degenerate in mass at about 1.9 GeV, LQCD calculations consistently show that the $J^{PC} = 1^{-+}$ nonet is the lightest. Predictions for the mass of this state have varied from 1.8 to 2.1 GeV, with an average about in the middle of these. Table V shows a number of these predictions made over the last several years. Most of these [19–23, 25] were made in the quenched approximation (no $q\bar{q}$ loops allowed in the calculation), while newer calculations [24, 26–28] are not quenched.

However, the masses in Table V may not be the best approximations to the hybrid masses. It has been noted [29] that Table V is not a very useful way of displaying the results. Rather, the mass needs to be correlated with the light-quark mass used in the calculation. This is usually represented as the pion mass. In Figure 1 are shown the predictions from the same groups as a function of the pion masses used in their calculations. In order to obtain the hybrid mass, one needs to extrapolate to the physical pion mass.

There are fewer predictions for the masses of the other

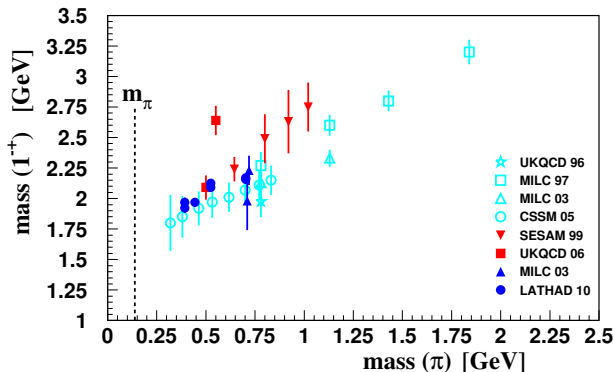


FIG. 1. (Color on line.) The mass of the $J^{PC} = 1^{-+}$ exotic hybrid as a function of the pion mass from lattice calculations. The open (cyan) symbols correspond to quenched calculations, while the solid (red and blue) symbols are unquenched: open (cyan) star [19], open (cyan) squares [20], open (cyan) upright triangles [24], open (cyan) circles [25], solid (red) downward triangles [21], solid (red) squares [26], solid (blue) upright triangles [24] and solid (blue) circles [28].

exotic-quantum number states. Bernard [20] calculated the splitting between the 0^{+-} and the 1^{-+} state to be about 0.2 GeV with large errors. A later calculation using a clover action [22] found a splitting of 0.270 ± 0.2 GeV. The SESAM collaboration [21] has one such calculation, the results of which are shown in Table VI. Recently,

Multiplet	J^{PC}	Mass
π_1	1^{-+}	$1.9 \pm 0.2 \text{ GeV}/c^2$
b_2	2^{+-}	$2.0 \pm 1.1 \text{ GeV}/c^2$
b_0	0^{+-}	$2.3 \pm 0.6 \text{ GeV}/c^2$

TABLE VI. Estimates of the masses of exotic quantum number hybrids [21].

Dudek [27] has carried out an exploratory study to calculate the entire light-meson spectrum. While this was not quenched, the three flavours of quarks all had the strange-quark mass ($m_\pi \sim 0.7$ GeV). The predicted spectrum shows a 1^{-+} nonet as well as a 0^{+-} and a 2^{+-} . With their assumptions, the 1^{-+} is the lightest and the other two exotic nonets are roughly degenerate in mass, and heavier than the 1^{-+} .

This calculation has recently been improved with several pions masses and two different lattice volumes [28]. Figure 2 shows these new results for the three exotic-quantum number states plotted as a function of the pion mass. The results appear relatively insensitive to the lattice volumes used and confirm that the 1^{-+} state is the lightest with the 0^{+-} and 2^{+-} nearly degenerate and a few hundred MeV higher in mass. In order to obtain the a mass prediction, these results need to be extrapolated to the physical pion mass.

Lattice calculations have also been performed to look for other exotic quantum number states. Bernard [20] included operators for a 0^{--} state, but found no evidence

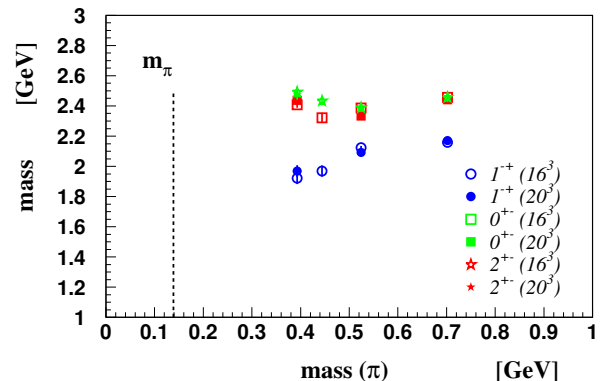


FIG. 2. (Color on line) The mass spectrum of the three exotic quantum number states [28]. The open figures are for a 16^3 spatial dimension lattice, while the solid are for a 20^3 spatial lattice. The (blue) circles are the mass of the 1^{-+} state, the (green) squares are the mass of the 0^{+-} state and the (red) stars are the 2^{+-} state.

for a state with these quantum numbers in their quenched calculation. Dudek [28] looked for both 0^{--} and 3^{--} states in their lattice data. They found some evidence for states with these quantum numbers, but the lightest masses were more than 2 GeV above the mass of the ρ meson.

D. Decay Modes

Currently, decays of hybrid mesons can only be calculated within models. Such models exist, having been developed to compute the decays of normal mesons. A basic feature of these is the so-called triplet-P-zero (3P_0) model. In the 3P_0 model, a meson decays by producing a $q\bar{q}$ pair with vacuum quantum numbers ($J^{PC} = 0^{++}$).

A detailed study by Ackleh, Barnes and Swanson [30] established that the 3P_0 amplitudes are dominant in most light-quark meson decays. They also determined the parameters in decay models by looking at the well known decays of mesons. This work was later extended to provide predictions for the decay of all orbital and radial excitations of mesons lighter than 2.1 GeV [31]. This tour-de-force in calculation has served as the backdrop against which most light-quark meson and hybrid candidates are compared.

The original calculations for the decays of hybrids in the flux-tube model were carried out by Isgur [17]. Within their model, Close and Page [32], confirmed the results and expanded the calculations to include additional hybrids. Using improved information about mesons and using simple harmonic oscillator (SHO) wave functions, they were able to compute the decay width of hybrid mesons. They also provided arguments for the selection rule that hybrids prefer to decay to an $L = 0$ and an $L = 1$ meson. The suppression of a pair of $L = 0$ mesons arises in the limit that the two mesons have the

Name	$\mathbf{J}^{\mathbf{PC}}$	Total Width MeV		Large Decays
		PSS	IKP	
π_1	1^{-+}	81 – 168	117	$b_1\pi, \rho\pi, f_1\pi, a_1\eta,$ $\eta(1295)\pi, K_1^A K, K_1^B K$
η_1	1^{-+}	59 – 158	107	$a_1\pi, f_1\eta, \pi(1300)\pi,$ $K_1^A K, K_1^B K$
η'_1	1^{-+}	95 – 216	172	$K_1^B K, K_1^A K, K^* K$
\bar{b}_0	0^{+-}	247 – 429	665	$\pi(1300)\pi, h_1\pi$
h_0	0^{+-}	59 – 262	94	$b_1\pi, h_1\eta, K(1460)K$
h'_0	0^{+-}	259 – 490	426	$K(1460)K, K_1^A K, h_1\eta$
b_2	2^{+-}	5 – 11	248	$a_2\pi, a_1\pi, h_1\pi$
h_2	2^{+-}	4 – 12	166	$b_1\pi, \rho\pi$
h'_2	2^{+-}	5 – 18	79	$K_1^B K, K_1^A K, K_2^* K, h_1\eta$

TABLE VII. Exotic quantum number hybrid width and decay predictions from reference [33]. The column labeled PSS (Page, Swanson and Szczepaniak) is from their model, while the IKP (Isgur, Karl and Paton) is their calculation of the model in reference [17]. The variations in width for PSS come from different choices for the masses of the hybrids. The K_1^A represents the $K_1(1270)$ while the K_1^B represents the $K_1(1400)$.

same inverse radius in the Simple Harmonic Oscillator wave functions. Thus, these decays are not strictly forbidden, but are suppressed depending on how close the two inverse radii are. This led to the often-quoted prediction for the decays of the π_1 hybrid given in equation 2.

$$\begin{aligned} \pi b_1 : \pi f_1 : \pi \rho : \eta \pi : \pi \eta' \\ = \\ 170 : 60 : 5 - 20 : 0 - 10 : 0 - 10 \end{aligned} \quad (2)$$

The current predictions for the widths of exotic-quantum-number hybrids are based on model calculations by Page *et al.* [33] for which the results are given in Table VII. They also computed decay rates for the hybrids with normal $q\bar{q}$ quantum numbers (results in Table VIII). While a number of these states are expected to be broad (in particular, most of the 0^{+-} exotic nonet), states in both the 2^{+-} and the 1^{-+} nonets are expected to have much narrower widths. The expected decay modes involve daughters that in turn decay. Thus making the overall reconstruction and analysis of these states much more complicated than simple two-pseudoscalar decays.

For the non-exotic quantum numbers states, it will be even more difficult. They are likely to mix with nearby normal $q\bar{q}$ states, complicating the expected decay pattern for both the hybrid and the normal mesons. However, the decays in Table VIII can be used as a guideline to help in identifying these states. In searches for hybrid mesons, the nonets with exotic quantum numbers provide the cleanest environment in which to search for these objects.

Close and Thomas [34] reexamined this problem in terms of work on hadronic loops in the $c\bar{c}$ sector by Barnes and Swanson [35]. They conclude that in the

limit where all mesons in a loop belong to a degenerate subset, vector hybrid mesons remain orthogonal to the $q\bar{q}$ states ($J^{PC} = 1^{--} {}^3S_1$ and 3D_1) and mixing may be minimal. Thus, the search for hybrids with vector $q\bar{q}$ quantum numbers may not be as difficult as the other non-exotic quantum number hybrids.

Particle	$\mathbf{J}^{\mathbf{PC}}$	Total Width MeV		Large Decays
		PSS	IKP	
ρ_1	1^{--}	70 – 121	112	$a_1\pi, \omega\pi, \rho\pi$
ω_1	1^{--}	61 – 134	60	$\rho\pi, \omega\eta, \rho(1450)\pi$
ϕ_1	1^{--}	95 – 155	120	$K_1^B K, K^* K, \phi\eta$
a_1	1^{++}	108 – 204	269	$\rho(1450)\pi, \rho\pi, K^* K$
h_1	1^{++}	43 – 130	436	$K^* K, a_1\pi$
h'_1	1^{++}	119 – 164	219	$K^*(1410)K, K^* K$
π_0	0^{-+}	102 – 224	132	$\rho\pi, f_0(1370)\pi$
η_0	0^{-+}	81 – 210	196	$a_0(1450)\pi, K^* K$
η'_0	0^{-+}	215 – 390	335	$K_0^* K, f_0(1370)\eta, K^* K$
b_1	1^{+-}	177 – 338	384	$\omega(1420)\pi, K^* K$
h_1	1^{+-}	305 – 529	632	$\rho(1450)\pi, \rho\pi, K^* K$
h'_1	1^{+-}	301 – 373	443	$K^*(1410)K, \phi\eta, K^* K$
π_2	2^{-+}	27 – 63	59	$\rho\pi, f_2\pi$
η_2	2^{-+}	27 – 58	69	$a_2\pi$
η'_2	2^{-+}	38 – 91	69	$K_2^* K, K^* K$

TABLE VIII. Non-exotic quantum number hybrid width and decay predictions from reference [33]. The column labeled PSS (Page, Swanson and Szczepaniak) is from their model, while the IKP (Isgur, Karl and Paton) is their calculation of the model in reference [17]. The variations in width for PSS come from different choices for the masses of the hybrids. The K_1^A represents the $K_1(1270)$ while the K_1^B represents the $K_1(1400)$.

Almost all models of hybrid mesons predict that they will not decay to identical pairs of mesons. Many also predict that decays to pairs of $L = 0$ mesons will be suppressed, leading to decays to an $(L = 0)(L = 1)$ pair as the favored hybrid decay mode. Page [36] undertook a study of these models of hybrid decay that included “TE hybrids” (with a transverse electric constituent gluon) in the bag model as well as “adiabatic hybrids” in the flux-tube model (hybrids in the limit where quarks move slowly with respect to the gluonic degrees of freedom). In such cases, the decays to pairs of orbital angular momentum $L = 0$ (S -wave) mesons were found to vanish. In both cases, it had been noted that this was true when the quark and the antiquark in the hybrid’s daughters have identical constituent masses with the same S -wave spatial wave functions, and the quarks are non-relativistic. In order to understand this, Page looked for an underlying symmetry that could be responsible for this. He found that symmetrization of connected decay diagrams (see Figure 3(a)) where the daughters are identical except for flavor and spin vanish when equation 3 is satisfied.

$$C_A^0 P_A = (-1)^{(S_A + S_{q\bar{q}} + 1)} \quad (3)$$

For meson A decaying to daughters B and C , C_A^0 is the

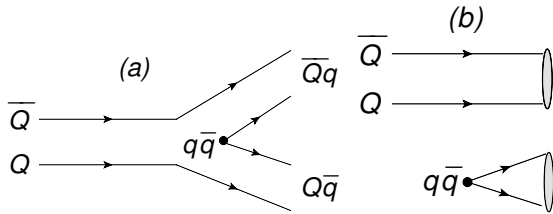


FIG. 3. (a) shows a connected decay diagram where the decay can be suppressed. (b) is an example of a disconnected diagram where the decay is not suppressed..

C-parity of the neutral isospin member of the decaying meson A , P_A is its parity and S_A is its intrinsic spin. $S_{q\bar{q}}$ is the total spin of the created pair. In the non-relativistic limit, $S_{q\bar{q}} = 1$. For non-connected diagrams (Figure 3(b)), he found no such general rules, so the vanishing of the decays occur to the extent that the non-connected diagrams are not important.

As an example of this, consider A to be the π_1 hybrid. It has $C_A^0 = +1$, $P_A = -1$ and $S_A = +1$, thus the left-hand side of equation 3 is -1 . The right-hand side is $(-1)^3 = -1$. The decay to pairs of mesons with the same internal angular momentum is suppressed to the extent that the disconnected diagram in Figure 3(b) is not important. In a later study, Close and Dudek [37] found that some of these decays could be large because the π and ρ wave functions were not the same.

While it has been historically difficult to compute decays on the lattice, a first study of the decay of the π_1 hybrid has been carried out by McNeile [26, 38]. In order to do this, they used a technique where they put a given decay channel at roughly the same energy as the decaying state. Thus, the decay is just allowed and conserves energy in a two-point function. In this way, they are able to extract the ratio of the decay width over the decay momentum, and find

$$\begin{aligned}\Gamma(\pi_1 \rightarrow b_1\pi)/k &= 0.66 \pm 0.20 \\ \Gamma(\pi_1 \rightarrow f_1\pi)/k &= 0.15 \pm 0.10\end{aligned}$$

which they note corresponds to a total decay width larger than 0.4 GeV for the π_1 . As a check of their procedure, they carry out a similar calculation for $b_1 \rightarrow \omega\pi$ where they obtain $\Gamma/k \sim 0.8$, which leads to $\Gamma(b_1 \rightarrow \omega\pi) \sim 0.22$ GeV. This is about a factor of 1.6 larger than the experimental width.

Burns and Close [39] examined these lattice decay results and made comparisons to what had been found in flux-tube model calculations. In Table IX are shown their comparison between flux-tube calculations for the width of the π_1 and the decay width from the lattice. They note that in reference [26], an assumption was made that Γ/k does not vary with the quark mass, and the resulting linear extrapolation leads to the large width in Table IX. They argue that the flux-tube model has been tested over a large range of k , where it accurately predicts the decays of mesons and baryons. Quoting them, “The successful

phenomenology of this and a wide range of other conventional meson decays relies on momentum-dependent form factors arising from the overlap of hadron wave functions. The need for such form factors is rather general, empirically supported as exclusive hadron decay widths do not show unrestricted growth with phase space.” Based on this, they carried out a comparison of the transition amplitudes computed for $k = 0$ (the lattice case). They found excellent agreement between the lattice and the flux-tube calculations. Thus, their concern that the extrapolation may be overestimating decay widths may be valid.

	IKP [17]	IKP [32]	Lattice [26]
	1.9 GeV	2.0 GeV	2.0 GeV
$\Gamma(\pi_1 \rightarrow b_1\pi)_S$	100	70	400 ± 120
$\Gamma(\pi_1 \rightarrow b_1\pi)_D$	30	30	
$\Gamma(\pi_1 \rightarrow f_1\pi)_S$	30	20	90 ± 60
$\Gamma(\pi_1 \rightarrow f_1\pi)_D$	20	25	

TABLE IX. Decay widths as computed in the flux-tube model (IKP) compared to the lattice calculations. (Table reproduced from reference [39].)

While the model calculations provide a good guide in looking for hybrids, there are often symmetries that can suppress or enhance certain decays. Chung and Klempt [40] noted one of these for decays of a $J^{PC} = 1^{-+}$ state into $\eta\pi$ where the η and π have relative angular momentum of $L = 1$. In particular, in the limit where the η is an SU(3) octet, the $\eta\pi$ in a p -wave must be in an antisymmetric wave function. In order to couple this to an octet (hybrid) meson, the hybrid must also be antisymmetric. This implies it must be a member of the 8_2 octet. However, the SU(3) Clebsch-Gordan coefficient for $8_2 \rightarrow \eta_8\pi$ is zero. Thus, the decay is forbidden.

However, by similar arguments, they showed that it can couple to the $10 \oplus 10$ representation of SU(3). A representation that contains multiquark ($qq\bar{q}\bar{q}$) objects (see Section II E). Similarly, for the singlet (η') in a p -wave, $\eta(1)\pi$, the coupling to an octet is not suppressed.

To the extent that the η is octet and the η' is singlet, a 1^{-+} state that decays to $\eta\pi$ and not $\eta'\pi$ cannot be a hybrid, while one that decays to $\eta'\pi$ and not $\eta\pi$ is a candidate for a 1^{-+} hybrid meson. Our current understanding of the pseudoscalar mixing angle is that it is between -10° and -20° [1], thus the assumption on the nature of the η and η' is not far off. However, as far as we know, the pseudoscalar mesons are the only nonet that is close to pure SU(3) states, all others tend to be close to ideal mixing. A case where the higher mass state is nearly pure $s\bar{s}$. Thus, this suppression would not be expected for decays to higher mass nonets.

E. Multiquark states

As noted in Section I, exotic quantum numbers can arise from other quark-gluon systems as well. While it is possible for glueballs to have exotic quantum numbers, the masses are expected to be above 3 GeV [41]. Four-quark states ($qq\bar{q}\bar{q}$) can be constructed using SU(3) symmetry. The qq system is a combination of a $\bar{3}$ and a 6 under SU(3), leading to possible four-quark multiplets as singlets, octets, decuplets and a 27-plet. However, Jaffe [42] noted that because the decays of these objects were super-allowed, that the states would not exist. Klempt [3] note that in the bag model, the 1^{-+} (qq)($\bar{q}\bar{q}$) is expected to be around 1.7 GeV and observe that the QSSR predictions may be lower. However, they go on to argue that (qq)($\bar{q}\bar{q}$) systems will not bind without additional $q\bar{q}$ forces, and feel that it is unlikely that these states exist.

III. EXPERIMENTAL RESULTS

A. Production processes

Data on exotic-quantum-number mesons have come from both diffractive production using incident pion beams and from antiproton annihilation on protons and neutrons. Diffractive production is schematically shown in Figure 4. A pion beam is incident on a proton (or nuclear) target, which recoils after exchanging something in the t -channel. The process can be written down in the reflectivity basis [43] in which the production factorizes into two non-interfering amplitudes—positive reflectivity ($\epsilon = +$) and negative reflectivity ($\epsilon = -$). The absolute value of the spin projection along the z -axis is M , and is taken to be either 0 or 1 (it is usually assumed that contributions from M larger than 1 are small and can be ignored[44]). It can be shown in this process that naturality of the exchanged particle can be determined by ϵ . Natural parity exchange (n.p.e.) corresponds to J^P s of $0^+, 1^-, 2^+, \dots$, while unnatural parity exchange (u.p.e.) corresponds to J^P of $0^-, 1^+, 2^-, \dots$.

For a state which is observed in more than one decay mode, one would expect that the production mechanism (M^ϵ) would be the same for all decay modes. If not, this could be indicative of more than one state being observed, or possible problems in the analysis that are not under control.

In antiproton-nucleon annihilation, there are a number of differences between various annihilation processes. For the case of $\bar{p}p$, the initial state is a mixture of isospin $I = 0$ and $I = 1$. For $\bar{p}n$ annihilation, the initial state is pure $I = 1$. For annihilation at rest, the initial state is dominated by atomic S-waves. In particular, 1S_0 and 3S_1 atomic states, which have $J^{PC} = 0^{-+}$ and 1^{--} respectively (with a small admixture of P states). For annihilation in flight, the number of initial states is much larger and it may no longer make sense to try and parametrize

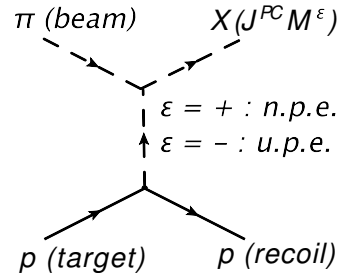


FIG. 4. The diffractive production process showing an incident pion (π beam) incident on a proton (p target) where the exchange has z -component on angular momentum M and reflectivity ϵ . The final state consists of a proton (p recoil) and a state X of given J^{PC} produced by an exchange M^ϵ . For positive reflectivity, the t -channel is a natural parity exchange (n.p.e.), while for negative reflectivity, it is unnatural parity exchange (u.p.e.). (This diagram was produced using the JaxoDraw package [45].)

the initial system in terms of atomic states.

The combination of initial isospin and final state particles may lead to additional selection rules that restrict the allowed initial states. In the case of $\bar{p}p \rightarrow \eta\pi^0\pi^0$, the annihilation is dominated by 1S_0 initial states ($J^{PC} = 0^{-+}$). For the case of $\bar{p}n \rightarrow \eta\pi^0\pi^-$, quantum numbers restrict this annihilation to occur from the 3S_1 initial states ($J^{PC} = 1^{--}$). Thus, one may see quite different final states from the two apparently similar reactions.

B. The $\pi_1(1400)$

The first reported observation of an exotic quantum number state came from the GAMS experiment which used a 40 GeV/c π^- to study the reaction $\pi^-p \rightarrow p\eta\pi^-$. They reported a $J^{PC} = 1^{-+}$ state in the $\eta\pi^-$ system which they called the $M(1405)$ [46]. The $M(1405)$ had a mass of 1.405 ± 0.020 GeV and a width of 0.18 ± 0.02 GeV. Interestingly, an earlier search in the $\eta\pi^0$ channel found no evidence of an exotic state [47]. At KEK, results were reported on studies using a 6.3 GeV/c π^- beam where they observed a 1^{-+} state in the $\eta\pi^-$ system with a mass of 1.3431 ± 0.0046 GeV and a width of 0.1432 ± 0.0125 GeV [48]. However, there was concern that this may have been leakage from the $a_2(1320)$. The VES collaboration reported intensity in the 1^{-+} $\eta\pi^-$ wave as well as rapid phase motion between the a_2 and the exotic wave [49] (see Figure 5). The exotic wave was present in the $M^\epsilon = 1^+$ (natural parity) exchange, but not in the 0^- and 1^- (unnatural parity) exchange. They could fit the observed $J^{PC} = 1^{-+}$ intensity and the phase motion with respect to the $a_2(1320)$ using a Breit-Wigner distribution (mass of 1.316 ± 0.012 GeV and width of 0.287 ± 0.025 GeV). However, they stopped short of claiming an exotic resonance, as they could not unambiguously establish the nature of the exotic wave [50]. In a later analysis of the $\eta\pi^0$ system, they claim that the

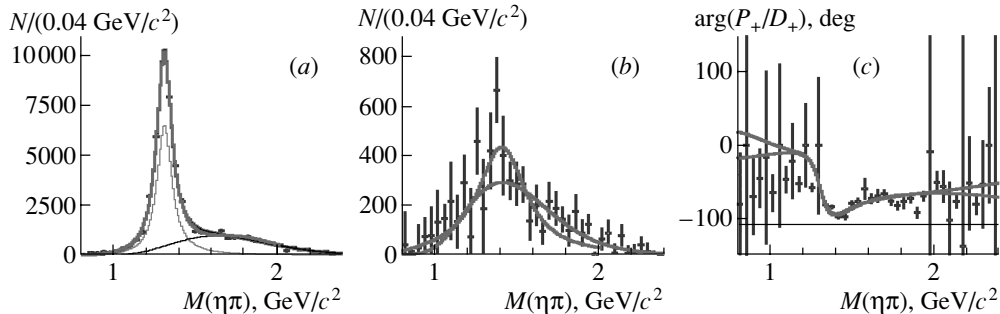


FIG. 5. The results of a partial-wave analysis of the $\eta\pi^-$ final state from VES. (a) shows the intensity in the 2^{++} partial wave, (b) shows the intensity in the 1^{-+} partial wave and (c) shows the relative phase between the waves. (Figure reproduced from reference [51].)

peak near 1.4 GeV can be understood without requiring an exotic quantum number meson [51].

The E852 collaboration used 18 GeV/c π^- beams to study the reaction $\pi^- p \rightarrow p\eta\pi^-$. They reported the observation of a 1^{-+} state in the $\eta\pi^-$ system [52]. E852 found this state only produced in natural parity exchange ($M^\epsilon = 1^+$). They measured a mass of $1.37 \pm 0.016^{+0.050}_{-0.030}$ GeV and a width of $0.385 \pm 0.040^{+0.065}_{-0.105}$ GeV. While the observed exotic signal was only a few percent of the dominant $a_2(1320)$ strength, they noted that its interference with the a_2 provided clear evidence of this state. When their intensity and phase-difference plots were compared with those from VES [49], they were identical. These plots (from E852) are reproduced in Figure 6.

The exotic π_1 state was confirmed by the Crystal Barrel Experiment which studied antiproton-neutron annihilation at rest in the reaction $\bar{p}n \rightarrow \eta\pi^-\pi^0$ [53]. The Dalitz plot for this final state is shown in Figure 7 where bands for the $a_2(1320)$ and $\rho(770)$ are clearly seen. They reported a 1^{-+} state with a mass of $1.40 \pm 0.020 \pm 0.020$ GeV and a width of $0.310 \pm 0.050^{+0.050}_{-0.030}$ GeV. While the signal is not obvious in the Dalitz plot, if one compares the difference between a fit to the data without and with the $\pi_1(1400)$, a clear discrepancy is seen when the $\pi_1(1400)$ is not included (see Figure 8). While the $\pi_1(1400)$ was only a small fraction of the $a_2(1320)$ in the E852 measurement [52], Crystal Barrel observed the two states produced with comparable strength.

Crystal Barrel also studied the reaction $\bar{p}p \rightarrow \eta\pi^0\pi^0$ [54]. Here, a weak signal was observed for the $\pi_1(1400)$ (relative to the $a_2(1320)$) with a mass of 1.360 ± 0.025 GeV and a width of 0.220 ± 0.090 GeV. In $I = 0$ $\bar{p}p$ annihilations, the $a_2(1320)$ is produced strongly from the 1S_0 atomic state. However, $\bar{p}n$ is isospin 1 and 1S_0 state is forbidden. Thus, the strong a_2 production from $\bar{p}p$ is suppressed in $\bar{p}d$ annihilations—making the $\pi_1(1400)$ production appear enhanced relative to the $a_2(1320)$ in the latter reaction.

An analysis of E852 data for the reaction $\pi^- p \rightarrow n\eta\pi^0$ found evidence for the exotic 1^{-+} partial wave, but were

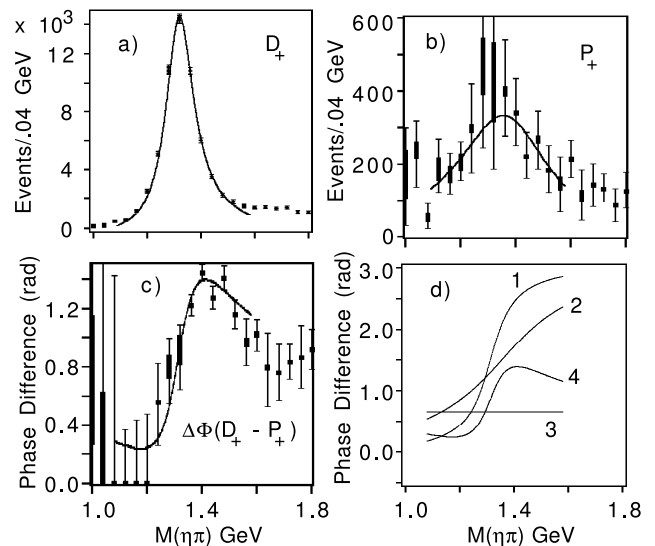


FIG. 6. The $\pi_1(1400)$ as observed in the E852 experiment [52]. (a) shows the intensity of the $J^{PC} = 2^{++}$ partial wave as a function of $\eta\pi$ mass. The strong signal is the $a_2(1320)$. (b) shows the intensity of the 1^{-+} wave as a function of mass, while (c) shows the phase difference between the 2^{++} and 1^{-+} partial waves. In (d) are shown the phases associated with (1) the $a_2(1320)$, (2) the $\pi_1(1400)$, (3) the assumed flat background phase and (4), the difference between the (1) and (2). (This figure is reproduced from reference [52].)

unable to describe it as a Breit-Wigner-like $\pi_1(1400)$ $\eta\pi^0$ resonance [55]. However, a later analysis by the E852 collaboration of the same final state confirmed their earlier observation of the $\pi_1(1400)$ [56]. E852 found a mass of $1.257 \pm 0.020 \pm 0.025$ GeV and a width of $0.354 \pm 0.064 \pm 0.058$ GeV with the $\pi_1(1400)$ produced via natural parity exchange ($M^\epsilon = 1^+$).

The $\pi_1(1400)$ was also reported in $\bar{p}p$ annihilation into four-pion final states by both Obelix [57] and Crystal Barrel [58] (conference proceedings only). They both observed the $\pi_1(1400)$ decaying to $\rho\pi$ final states, however

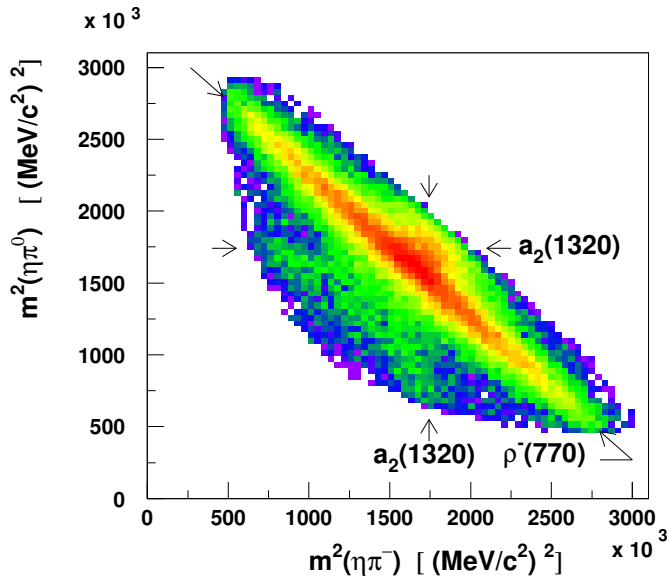


FIG. 7. (Color on line.) The Dalitz plot of $m^2(\eta\pi^0)$ versus $m^2(\eta\pi^-)$ for the reaction $\bar{p}n \rightarrow \eta\pi^-\pi^0$ from the Crystal Barrel experiment [53]. The bands for the $a_2(1320)$ are clearly seen in both $\eta\pi^0$ and $\eta\pi^-$, while the $\rho(770)$ is seen in the $\pi^0\pi^-$ invariant mass.

there is some concern about the production mechanism. The $\eta\pi$ signal arises from annihilation from the 3S_1 initial state, while the signal in $\rho\pi$ come from the 1S_0 initial state. Thus, it is unlikely that the exotic state seen in $\eta\pi$ and that seen in $\rho\pi$ are the same. The origin of these may not be due to an exotic resonance, but rather some re-scattering mechanism that has not been properly accounted for.

Interpretation of the $\pi_1(1400)$ has been problematic. Its mass is lower than most predicted values from models, and its observation in only a single decay mode ($\eta\pi$) is not consistent with models of hybrid decays. Donachie and Page showed that the $\pi_1(1400)$ could be an artifact of the production dynamics. They demonstrated that it is possible to understand the $\pi_1(1400)$ peak as a consequence of the $\pi_1(1600)$ (see Section III C) interfering with a non-resonant Deck-type background with an appropriate relative phase [59].

Szczepaniak [60] considered a model in which t -channel forces could give rise to a background amplitude which could be responsible for the observed $\pi_1(1400)$. In this model, meson-meson interactions which respected chiral symmetry were used to construct the $\eta\pi$ p -wave interaction much like the $\pi\pi$ s -wave interaction gives rise to the σ meson. They claimed that the $\pi_1(1400)$ was not a QCD bound state, but rather dynamically generated by meson exchange forces.

Chung [40] noted that in the limit of the η being a pure octet state, that the decay of an octet 1^{-+} state to an $\eta\pi$ p -wave is forbidden. Such a decay can only come from a decuplet state. Given that the pseudoscalar mixing angle

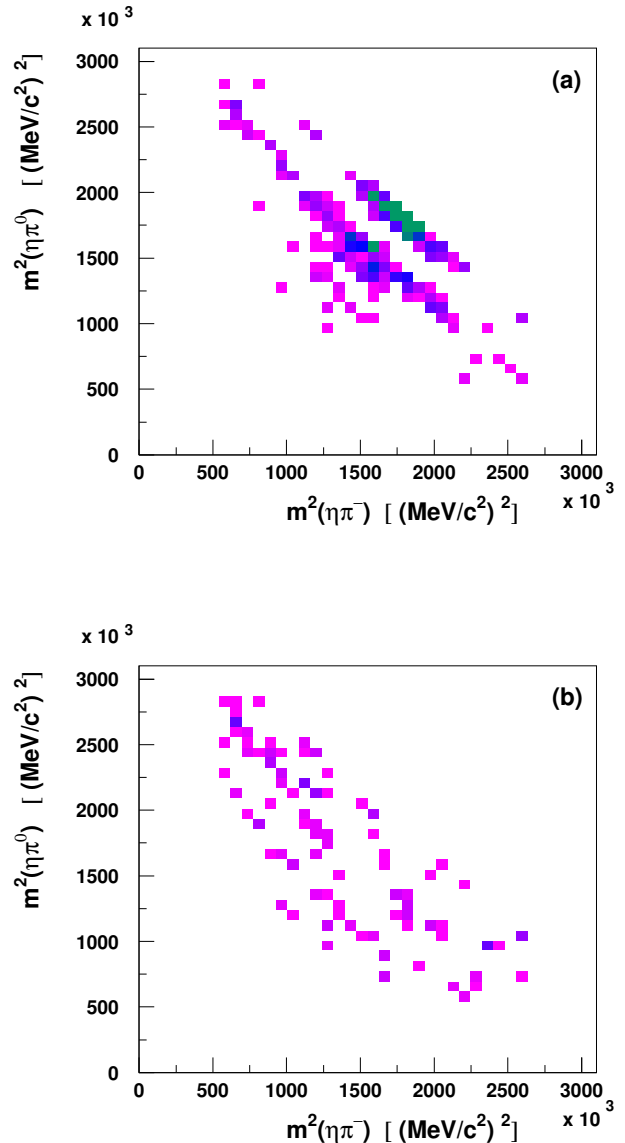


FIG. 8. (Color on line.) The difference between the fit and the data in the Dalitz plot of $m^2(\eta\pi^0)$ versus $\eta\pi^-$ for the reaction $\bar{p}n \rightarrow \eta\pi^-\pi^0$ from the Crystal Barrel experiment [53]. (a) Does not include the $\pi_1(1400)$ while (b) does include the $\pi_1(1400)$. There are clear systematic discrepancies present in (a) that are not present when the $\pi_1(1400)$ is included.

for the η and η' are close to this assumption, they argue that the $\pi_1(1400)$ is $qq\bar{q}\bar{q}$ in nature.

While the interpretation of the $\pi_1(1400)$ is not clear, most analyses agree that there is intensity in the 1^{-+} wave near this mass. A summary of all reported masses and widths for the $\pi_1(1400)$ are given in Table X. All are reasonably consistent, and even the null observations of VES and E852 data concur that there is strength near 1.4 GeV in the J^{PC} exotic wave.

Mode	Mass (GeV)	Width (GeV)	Experiment	Reference
$\eta\pi^-$	1.405 ± 0.020	0.18 ± 0.02	GAMS	[46]
$\eta\pi^-$	1.343 ± 0.0046	0.1432 ± 0.0125	KEK	[48]
$\eta\pi^-$	1.37 ± 0.016	0.385 ± 0.040	E852	[52]
$\eta\pi^0$	1.257 ± 0.020	0.354 ± 0.064	E852	[56]
$\eta\pi^-$	1.40 ± 0.020	0.310 ± 0.050	CBAR	[53]
$\eta\pi^0$	1.36 ± 0.025	0.220 ± 0.090	CBAR	[54]
$\rho\pi$	1.384 ± 0.028	0.378 ± 0.058	Obelix	[57]
$\rho\pi$	~ 1.4	~ 0.4	CBAR	[58]
$\eta\pi$	1.351 ± 0.030	0.313 ± 0.040	PDG	[1]

TABLE X. Reported masses and widths of the $\pi_1(1400)$ from the GAMS, KEK, E852, Crystal Barrel (CBAR) and Obelix experiment. Also reported is the 2008 PDG average for the state.

C. The $\pi_1(1600)$

While the low mass, and single observed decay mode, of the $\pi_1(1400)$ have presented some problems in understanding its nature, a second $J^{PC} = 1^{-+}$ state may be less problematic. The $\pi_1(1600)$ has been observed in diffractive production using incident π^- beams where its mass and width have been reasonably stable over several experiments and the decay modes. It may also have been observed in $\bar{p}p$ annihilation. Positive results have been reported from VES, E852, COMPASS and others. These are discussed below in approximate chronological order.

In addition to their study of the $\eta\pi^-$ system, the VES collaboration also examined the $\eta'\pi^-$ system. Here they observed a $J^{PC} = 1^{-+}$ partial wave with intensity peaking at a higher mass than the $\pi_1(1400)$ [49]. However, as with the $\eta\pi^-$ system, they did not claim the discovery of an exotic-quantum-number resonance. VES later reported a combined study of the $\eta'\pi^-$, $f_1\pi^-$ and $\rho^0\pi^-$ final states [61], and reported a “resonance-like structure” with a mass of 1.62 ± 0.02 GeV and a width of 0.24 ± 0.05 GeV decaying into $\rho^0\pi^-$. They also noted that the wave with $J^{PC} = 1^{-+}$ dominates in the $\eta'\pi^-$ final state, peaking near 1.6 GeV and observed a small 1^{-+} signal in the $f_1\pi^-$ final state.

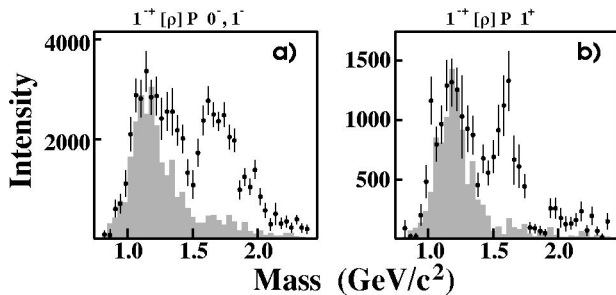


FIG. 9. The production of the 1^{-+} partial wave as seen in the $\pi^+\pi^-\pi^-$ final state by E852. (a) shows the unnatural parity exchange ($M^\epsilon = 0^-, 1^-$) while (b) shows the natural parity exchange ($M^\epsilon = 1^+$). (Figure reproduced from reference [62].)

Using an 18 GeV/c π^- beam incident on a proton target, the E852 collaboration carried out a partial wave analysis on the $\pi^+\pi^-\pi^-$ final state [62, 63]. They saw both the $\rho^0\pi^-$ and $f_2(1270)\pi^-$ intermediate states and observed a $J^{PC} = 1^{-+}$ state which decayed to $\rho\pi$, the $\pi_1(1600)$. The $\pi_1(1600)$ was produced in both natural and unnatural parity exchange ($M^\epsilon = 1^+$ and $M^\epsilon = 0^-, 1^-$) with similar strengths in all three exchange mechanisms (see Figure 9). In their analysis, they only considered the natural parity exchange. There, they found the $\pi_1(1600)$ to have a mass of $1.593 \pm 0.08_{-0.047}^{+0.029}$ GeV and a width of $0.168 \pm 0.020_{-0.012}^{+0.150}$ GeV. In Figure 10 are shown the intensity of the 1^{-+} and 2^{-+} ($\pi_2(1670)$) partial waves as well as their phase difference. The phase difference can be reproduced by two interfering Breit-Wigner distributions and a flat background.

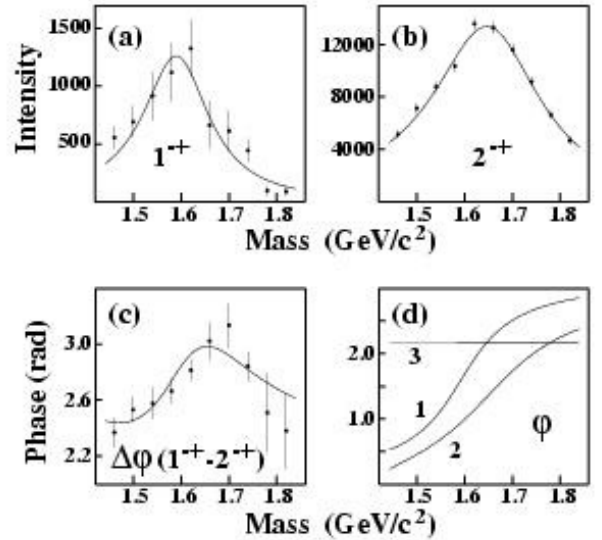


FIG. 10. The results of a PWA to the $\pi^+\pi^-\pi^-$ final state from E852. (a) shows the intensity of the $J^{PC} = 1^{-+}$ wave, (b) shows the 2^{-+} and (c) shows the phase difference between the two. The solid curves are fits to two interfering Breit-Wigner distributions. In (d) are shown the phases of the two Breit-Wigner distributions and (1,2) and a flat background phase (3) that combine to make the curve in (c). (Figure reproduced from reference [62].)

VES also reported on the $\omega\pi^-\pi^0$ final state [64, 65]. In a combined analysis of the $\eta'\pi^-$, $b_1\pi$ and $\rho^0\pi^-$ final states, they reported the $\pi_1(1600)$ state with a mass of 1.61 ± 0.02 GeV and a width of 0.29 ± 0.03 GeV that was consistent with all three final states. To the extent that they observed these states, they also observed all three final state produced in natural parity exchange ($M^\epsilon = 1^+$). They were also able to report relative branching ratios for the three final states as given in equation 4.

$$b_{1\pi} : \eta'\pi : \rho\pi : = 1 : 1 \pm 0.3 : 1.5 \pm 0.5 \quad (4)$$

However, there were some issues with the $\rho\pi$ final state.

Rather than limiting the rank of the density matrix as was done in [62, 63], they did not limit it. This allowed for a more general fit that might be less sensitive to acceptance affects. In this model, they did not observe any significant structure in the 1^{-+} $\rho\pi$ partial wave above 1.4 GeV. However, by looking at how other resonances were produced, they were able to isolate a coherent part of the density matrix from which they found a statistically significant 1^{-+} partial wave peaking near 1.6 GeV. While VES was extremely careful not to claim the existence of the $\rho\pi$ decay of the $\pi_1(1600)$, in the case that it exists, they were able to obtain the rates given in equation 4.

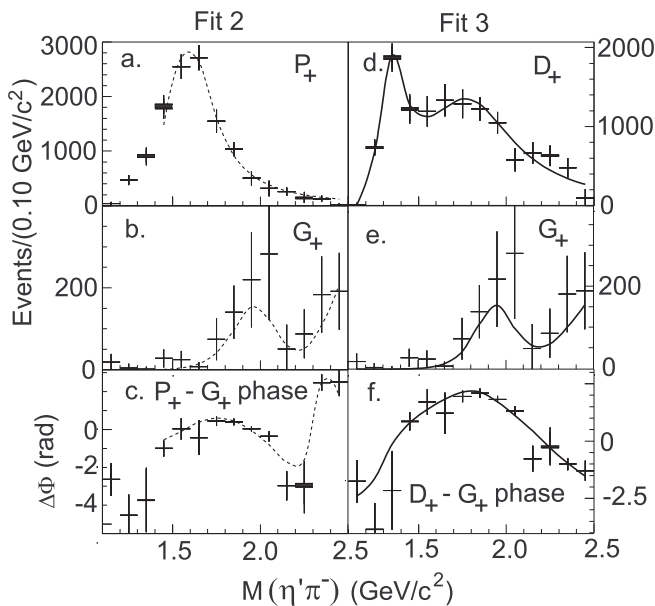


FIG. 11. Results from E852 on the $\eta'\pi^-$ final state. (a) shows the 1^{-+} partial wave, (b) shows the 4^{++} partial wave (an a_4) and (c) shows the phase difference between these. (d) shows the 2^{++} partial wave ($a_2(1320)$), while (e) shows the a_4 and (f) is the phase difference. (Figure reproduced from reference [66].)

In a follow-up analysis, E852 also studied the reaction $\pi^-p \rightarrow p\eta'\pi^-$ to examine the $\eta'\pi^-$ final state [66]. They observed, consistent with VES [49], that the dominant signal was the 1^{-+} exotic wave produced dominantly in the $M^\epsilon = 1^+$ channel, implying only natural parity exchange. They found the signal to be consistent with a resonance, the $\pi_1(1600)$ and found a mass of $1.597 \pm 0.010^{+0.045}_{-0.010}$ GeV and a width of $0.340 \pm 0.040 \pm 0.050$ GeV. The results of the E852 PWA are shown in Figure 11 where the P_+ wave is the 1^{-+} , the D_+ corresponds to the 2^{++} a_2 and the G_+ corresponds to the 4^{++} a_4 . Clear phase motion is observed between both the 2^{++} and 4^{++} wave and the 1^{-+} and the 4^{++} wave.

An analysis of Crystal Barrel data at rest for the reaction $\bar{p}p \rightarrow \omega\pi^+\pi^-\pi^0$ was carried by some members of the collaboration [67]. They reported evidence for the

$\pi_1(1600)$ decaying to $b_1\pi$ from both the 1S_0 and 3S_1 initial states, with the signal being stronger from the former. The total signal including both initial states, as well as decays with 0 and 2 units of angular momentum accounted for less than 10% of the total reaction channel. The mass and width were found consistent (within large errors) of the PDG value, and only results with the mass and width fixed to the PDG values were reported. Accounting for the large rate of annihilation to $\omega\pi^+\pi^-\pi^0$ of 13%, this would imply that $\bar{p}p \rightarrow \pi_1(1600)\pi$ accounts for several percent of all $\bar{p}p$ annihilations.

E852 also looked for the decays of the $\pi_1(1600)$ to $b_1\pi$ and $f_1\pi$. The latter was studied in the reaction $\pi^-p \rightarrow p\eta\pi^+\pi^-\pi^-$ with the f_1 being reconstructed in its $\eta\pi^+\pi^-$ decay mode [68]. The $\pi_1(1600)$ was seen via interference with both the 1^{++} and 2^{-+} partial waves. It was produced in via natural parity exchange ($M^\epsilon = 1^+$) and they found the $\pi_1(1600)$ to have a mass of $1.709 \pm 0.024 \pm 0.041$ GeV and a width of $0.403 \pm 0.080 \pm 0.115$ GeV. A second π_1 state was also observed in this reaction (see Section III D).

The $b_1\pi$ final state was studied by looking at the reaction $\pi^-p \rightarrow \omega\pi^-\pi^0p$, with the b_1 reconstructed in its $\omega\pi$ decay mode [69]. The $\pi_1(1600)$ was seen interfering with the 2^{++} and 4^{++} partial waves. In $b_1\pi$, they measured a mass of $1.664 \pm 0.008 \pm 0.010$ GeV and a width of $0.185 \pm 0.025 \pm 0.028$ GeV for the $\pi_1(1600)$. However, the production mechanism was seen to be a mixture of both natural and unnatural parity exchange, with the unnatural being stronger. As with the $f_1\pi$, they also observed a second π_1 state decaying to $b_1\pi$ (see Section III D).

final state	production (M^ϵ)	dominant
$\rho\pi$	$0^-, 1^-, 1^+$	npe \sim upe
$\eta'\pi$	1^+	npe
$f_1\pi$	1^+	npe
$b_1\pi$	$0^-, 1^-, 1^+$	upe $>$ npe

TABLE XI. The production mechanisms for the $\pi_1(1600)$ as seen in the E852 experiment. Also shown is whether the natural parity exchange (npe) or the unnatural parity exchange (upe) is stronger.

The fact that E852 observed the $\pi_1(1600)$ produced in different production mechanisms, depending on the final state, is somewhat confusing. A summary of the observed mechanisms is given in Table XI. In order to understand the variations in production, there either needs to be two nearly-degenerate $\pi_1(1600)$ s, or there is some unaccounted-for systematic problem in some of the analyses.

A follow-up analysis of E852 data used an order of magnitude larger data set and looked at the reactions $\pi^-p \rightarrow n\pi^+\pi^-\pi^-$ and $\pi^-p \rightarrow n\pi^-\pi^0\pi^0$. The group carried out a partial wave analysis for both the $\pi^+\pi^-\pi^-$ and the $\pi^-\pi^0\pi^0$ final states and found a solution that was consistent with both data sets [71]. In this later analysis, they carried out a systematic study of which

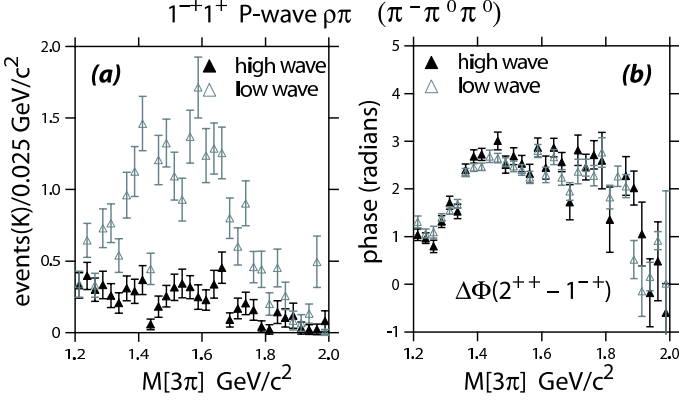


FIG. 12. The PWA solutions for the 1^{-+} partial wave for the $\pi^{-}\pi^0\pi^0$ final state (a) and its interference with the 2^{++} partial wave (b). See text for an explanation of the labels. (Figure reproduced from reference [71].)

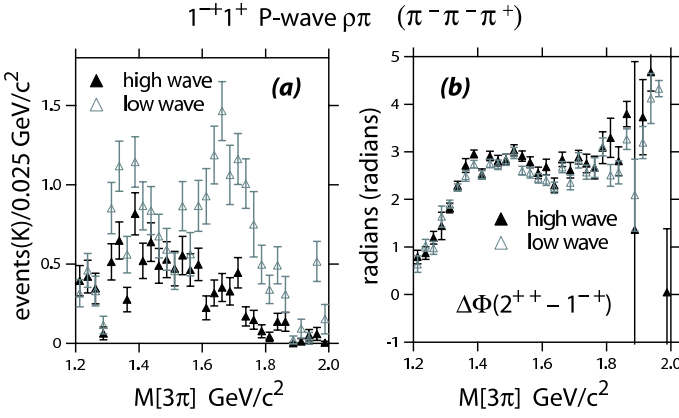


FIG. 13. The PWA solutions for the 1^{-+} partial wave for the $\pi^{+}\pi^{-}\pi^{-}$ final state (a) and its interference with the 2^{++} partial wave (b). See text for an explanation of the labels. (Figure reproduced from reference [71].)

partial waves were important in the fit. When they used the same wave set as in the E852 analysis [62, 63], they found the same solution showing a signal for the $\pi_1(1600)$ in both final states. However, when they allowed for more partial waves, they found that the signal for the $\pi_1(1600)$ went away. Figure 12 shows these results for the $\pi^{-}\pi^0\pi^0$ final state, while Figure 13 shows the results for the $\pi^{+}\pi^{-}\pi^{-}$ final state. In both figures, the “low wave” solution matches that from E852, while their “high wave” solution shows no intensity for the $\pi_1(1600)$ in either channel. One should note that the phase difference between the 2^{++} and the 1^{-+} waves are the same in both solutions.

A study was carried out to determine which of the additional waves in their “high wave” set were absorbing the intensity of the $\pi_1(1600)$. They found that the majority of this was due to the inclusion of the $\rho\pi$ decay of the $\pi_2(1670)$. The partial waves associated with the $\pi_2(1670)$ in both analyses are listed in Table XII. While the pro-

$\pi_2(1670)$ Decay	$M^\epsilon = 0^+$	$M^\epsilon = 1^+$		$M^\epsilon = 1^-$	
	L	H	L	H	L
$(f_2\pi)_S$	×	×	×	×	×
$(f_2\pi)_D$	×	×	×	×	
$[(\pi\pi)_S]_D$	×	×		×	
$(\rho\pi)_P$	×	×		×	
$(\rho\pi)_F$		×		×	
$(f_0\pi)_D$		×		×	

TABLE XII. The included decays of the $\pi_2(1670)$ in two analyses of the 3π final state. “L” is the wave set used in the E852 analysis [62, 63]. “H” is the wave set used in the higher statistics analysis [71].

duction from $M^\epsilon = 0^+$ is similar for both analyses, the E852 analysis only included the $\pi_2(1670)$ decaying to $f_2\pi$ in the $M^\epsilon = 1^+$ production. The high-statistics analysis included both $f_2\pi$ and $\rho\pi$ in both production mechanisms. The PDG [1] lists the two main decays of the $\pi_2(1670)$ as $f_2\pi$ (56%) and $\rho\pi$ (31%), so it seems odd to not include this latter decay in an analysis including the $\pi_2(1670)$. Figure 14 shows the results of removing the $\rho\pi$ decay from the “high wave” set for the $\pi^{+}\pi^{-}\pi^{-}$ final state. This decay absorbs a significant portion of the $\pi_1(1600)$ partial wave.

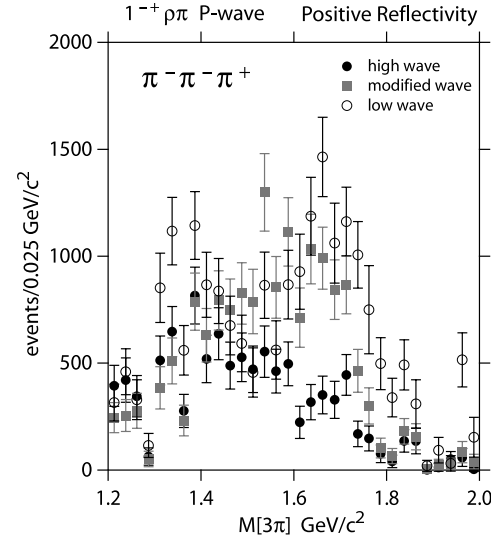


FIG. 14. The 1^{-+} intensity for the charged mode for the high-wave set (filled circles), the modified high-wave set (filled squares), and the low-wave set (open circles). In the modified high-wave set the two $\rho\pi$ decays of the $\pi_2(1670)$ were removed from the fit. (Figure reproduced from reference [71].)

The VES results have been summarized in a review of all their work on hybrid mesons [72]. This included an updated summary of the $\pi_1(1600)$ in all four final states, $\eta'\pi$, $\rho\pi$, $b_1\pi$ and $f_1\pi$. In the $\eta'\pi$ final state (Figure 15), they note that the 1^{-+} wave is dominant. While they were concerned about the nature of the higher-mass part of the 2^{++} spectrum ($a_2(1700)$ or background) they find that a resonant description of $\pi_1(1600)$ is possible in both

cases. For the case of the $b_1\pi$ final state (Figure 16), they find that the contribution of a $\pi_1(1600)$ resonance is required. In a combined fit to both the $\eta'\pi$ and $b_1\pi$ data, they find a mass of 1.56 ± 0.06 GeV and a width of 0.34 ± 0.06 GeV for the $\pi_1(1600)$. In the $f_1\pi$ final state (Figure 17), they find a resonant description of the the $\pi_1(1600)$ with a mass of 1.64 ± 0.03 GeV and a width of 0.24 ± 0.06 GeV which they note is compatible with their measurement in the previous two final states. They also note, that in contradiction with E852 [68], they find no significant 1^{-+} intensity above a mass of 1.9 GeV (see Section III D). For the $\rho\pi$ final state, they are unable to conclude that the $\pi_1(1600)$ is present.

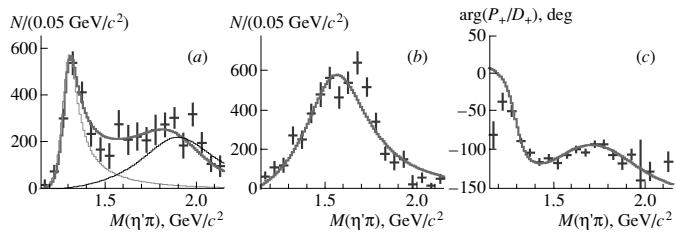


FIG. 15. The results of a partial wave analysis on the $\eta'\pi^-$ final state from VES. (a) shows the 2^{++} partial wave in $\omega\rho$, (b) shows the 1^{-+} partial wave in $b_1\pi$ and (c) shows the interference between them. (Figure reproduced from reference [72].)

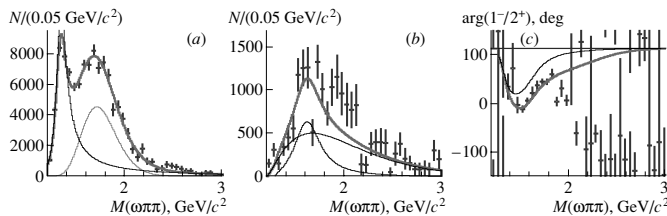


FIG. 16. The results of a partial wave analysis on the $b_1\pi$ final state from VES. (a) shows the 2^{++} partial wave, (b) shows the 1^{-+} partial wave and (c) shows the interference between them. (Figure reproduced from reference [72].)

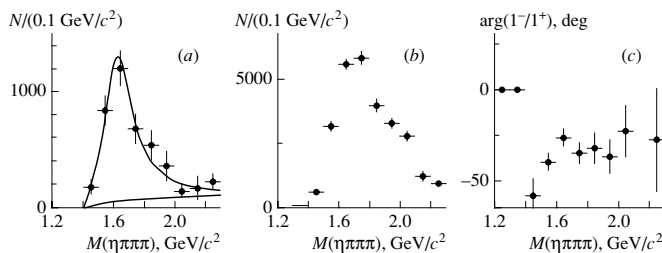


FIG. 17. The results of a partial wave analysis on the $f_1\pi$ final state from VES. (a) shows the 1^{++} partial wave, (b) shows the 1^{-+} partial wave and (c) shows the interference between them. (Figure reproduced from reference [72].)

They note that the partial-wave analysis of the $\pi^+\pi^-\pi^-$ system finds a significant contribution from the

$J^{PC} = 1^+$ wave in the $\rho\pi$ channel (2 to 3% of the total intensity). Some of the models in the partial-wave analysis of the exotic wave lead to the appearance of a peak near a mass of 1.6 GeV which resembles the $\pi_1(1600)$. However, the dependence of the size of this peak on the model used is significant [65]. They note that because the significance of the wave depends very strongly on the assumptions of coherence used in the analysis, the results for 3π final states on the nature of the $\pi_1(1600)$ are not reliable.

To obtain a limit on the branching fraction of $\pi_1(1600)$ decay to $\rho\pi$, they looked at their results of the production of the $\pi_1(1600)$ in the charge-exchange reaction to $\eta'\pi^0$ versus that of the $\eta'\pi^-$ final state. They conclude that the presence of the $\pi_1(1600)$ in $\eta'\pi^-$ and its absence in $\eta'\pi^0$ preclude the formation of the $\pi_1(1600)$ by ρ exchange. From this, they obtain the relative branching ratios for the $\pi_1(1600)$ as given in equation 5.

$$b_1\pi : f_1\pi : \rho\pi : \eta'\pi = 1.0 \pm .3 : 1.1 \pm .3 : < .3 : 1 \quad (5)$$

The CLAS experiment at Jefferson Lab studied the reaction $\gamma p \rightarrow \pi^+\pi^+\pi^-(n)_{miss}$ to look for the production of the $\pi_1(1600)$ [73]. The photons were produced by bremsstrahlung from a 5.7 GeV electron beam. While there was significant contributions from Baryon resonances in their data, they attempted to remove this by selective cuts on various kinematic regions. The results of their partial-wave analysis show clear signals for the $a_1(1270)$, the $a_2(1320)$ and the $\pi_2(1670)$, but show no evidence for the $\pi_1(1600)$ decaying into three pions. They place an upper limit of the production and subsequent decay of the $\pi_1(1600)$ to be less than 2% of the $a_2(1320)$.

The COMPASS experiment has reported their first study of the diffractively produced 3π final state [74, 75]. They used a 190 GeV/c beam of pions to study the reaction $\pi^-Pb \rightarrow \pi^-\pi^-\pi^+X$. In their partial-wave analysis of the 3π final state, they observed the $\pi_1(1600)$ with a mass of $1.660 \pm 0.010_{-0.064}^{+0}$ GeV and a width of $0.269 \pm 0.021_{-0.064}^{+0.042}$ GeV. The $\pi_1(1600)$ was produced dominantly in natural parity exchange ($M^\epsilon = 1^+$) although unnatural parity exchange also seemed to be required. However, the level was not reported. The wave set (in reference [75]) used appears to be somewhat larger than that used in the high-statistics study of the E852 data [71]. Thus, in the COMPASS analysis, the $\rho\pi$ decay of the $\pi_2(1670)$ does not appear to absorb the exotic intensity in their analysis. They also report on varying the rank of the fit with the $\pi_1(1600)$ and the results being robust against these changes. One point of small concern is that the mass and width that they extract for the $\pi_1(1600)$ are essentially identical to those for the $\pi_2(1670)$. For the latter, they observed a mass of $1.658 \pm 0.002_{-0.008}^{+0.024}$ GeV and a width of $0.271 \pm 0.009_{-0.024}^{+0.022}$ GeV. However, the strength of the exotic wave appears to be about 20% of the π_2 , thus feed through seems unlikely. Results from their partial-wave analysis are shown in Figure 19 which shows the signals

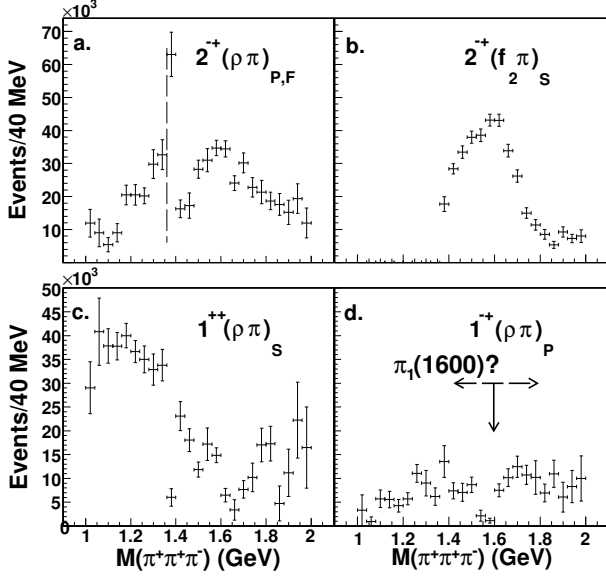


FIG. 18. The results of a partial-wave analysis photoproduction data of the 3π final state. Intensity is seen in the 2^{-+} partial wave, (a) and (b), as well as the 1^{++} partial wave (c). In the 1^{-+} exotic wave, (d), no intensity is observed. (Figure reproduced from reference [73].)

from the four dominant partial waves in their analysis (1^{++} , 2^{++} , 2^{-+} and 1^{-+}).

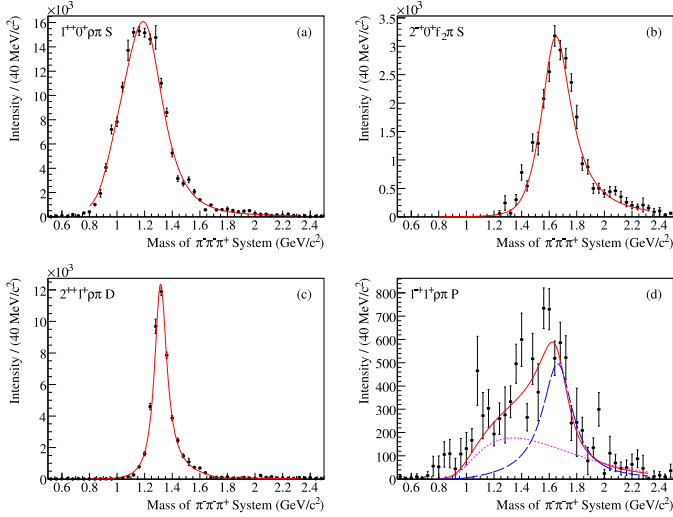


FIG. 19. (Color on line.) The intensity of the four dominant waves observed in the COMPASS experiment. (a) Shows the 1^{++} wave which is dominated by the $a_1(1270)$. (b) shows the 2^{-+} wave which is dominantly the $\pi_2(1670)$, while (c) is the 2^{++} wave, the $a_2(1320)$. (d) shows the exotic 1^{-+} wave. The solid (red) curves show fits to the corresponding resonances. In (d), the dashed (blue) curve is the $\pi_1(1600)$ while the dotted (magenta) curve is background. (Figure reproduced from reference [74].)

Table XIII summarizes the masses and widths found

for the $\pi_1(1600)$ in the four decay modes and from the experiments which have seen a positive result. While the $\eta'\pi$, $f_1\pi$ and $b_1\pi$ decay modes appear to be robust in the observation of a resonant $\pi_1(1600)$, there are concerns about the 3π final states. While we report these in the table, the results should be taken with some caution.

Mode	Mass (GeV)	Width (GeV)	Experiment	Reference
$\rho\pi$	1.593 ± 0.08	0.168 ± 0.020	E852	[62]
$\eta'\pi$	1.597 ± 0.010	0.340 ± 0.040	E852	[66]
$f_1\pi$	1.709 ± 0.024	0.403 ± 0.080	E852	[68]
$b_1\pi$	1.664 ± 0.008	0.185 ± 0.025	E852	[69]
$b_1\pi$	1.58 ± 0.03	0.30 ± 0.03	VES	[70]
$b_1\pi$	1.61 ± 0.02	0.290 ± 0.03	VES	[64]
$b_1\pi$	~ 1.6	~ 0.33	VES	[50]
$b_1\pi$	1.56 ± 0.06	0.34 ± 0.06	VES	[72]
$f_1\pi$	1.64 ± 0.03	0.24 ± 0.06	VES	[72]
$\eta'\pi$	1.58 ± 0.03	0.30 ± 0.03	VES	[70]
$\eta'\pi$	1.61 ± 0.02	0.290 ± 0.03	VES	[64]
$\eta'\pi$	1.56 ± 0.06	0.34 ± 0.06	VES	[72]
$b_1\pi$	~ 1.6	~ 0.23	CBAR	[67]
$\rho\pi$	1.660 ± 0.010	0.269 ± 0.021	COMPASS	[74]
all	$1.662^{+0.015}_{-0.011}$	0.234 ± 0.050	PDG	[1]

TABLE XIII. Reported masses and widths of the $\pi_1(1600)$ from the E852 experiment, the VES experiment and the COMPASS experiment. The PDG average from 2008 is also reported.

The models of hybrid decays predict rates for the decay of the π_1 hybrid. Equation 2 gives the predictions from reference [32]. A second model from reference [33] predicted the following rates for a $\pi_1(1600)$.

	πb_1	$\rho\pi$	πf_1	$\eta(1295)\pi$	K^*K
PSS	24	9	5	2	0.8
IKP	59	8	14	1	0.4

These can be compared to the results from VES in equation 5, which are in moderate agreement. The real identification of the $\pi_1(1600)$ as a hybrid will almost certainly involve the identification of other members of the nonet: the η_1 and/or the η'_1 , both of which are expected to have widths that are similar to the π_1 . For the case of the η_1 , the most promising decay mode may be the $f_1\eta$ as it involves reasonably narrow daughters.

D. The $\pi_1(2015)$

The E852 experiment has also reported a third π_1 state seen decaying to both $f_1\pi$ [68] and to $b_1\pi$ [69]. In the $f_1\pi$ final state, the $\pi_1(2015)$ is produced with $M^\epsilon = 1^+$ in conjunction with the $\pi_1(1600)$. The description of the 1^{-+} partial wave requires two poles. They report a mass of $2.001 \pm 0.030 \pm 0.092$ GeV and a width of $0.333 \pm 0.052 \pm 0.049$ GeV. VES also examined the $f_1\pi$ final state, and their intensity of the 1^{-+} partial wave above 1.9 GeV (see Figure 17) is not inconsistent with that of E852 [72]. However, VES made no comment on this nor have they claimed the existence of the $\pi_1(2015)$.

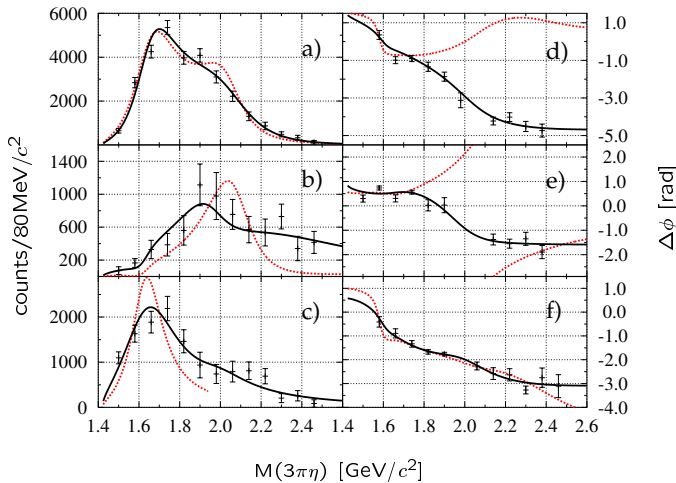


FIG. 20. (Color on line.) The $f_1\pi$ invariant mass from E852 [68]. (a) The 1^{++} partial wave ($a_1(1270)$), (b) the 2^{-+} partial wave ($\pi_2(1670)$) and (c) the exotic 1^{-+} partial wave. The dotted (red) curves show the fits of Breit-Wigner distributions to the partial waves. (d) shows the phase difference between the 2^{-+} and 1^{-+} partial waves, while (e) shows the difference between the 1^{++} and 1^{-+} partial waves. The dotted (red) curves show the results for a single π_1 state, the $\pi_1(1600)$. (f) shows the same phase difference as in (d), but the dotted (red) curve shows a fit with two poles in the 1^{-+} partial wave, the $\pi_1(1600)$ and the $\pi_1(2015)$. (Figure reproduced from reference [68].)

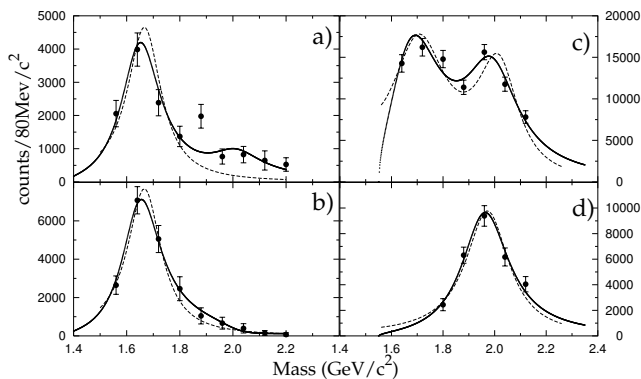


FIG. 21. The $b_1\pi$ invariant mass from the E852 experiment. (a) shows the 1^{-+} $b_1\pi$ partial wave produced in natural parity exchange ($M^\epsilon = 1^+$) while (b) shows the 1^{-+} $b_1\pi$ partial wave produced in unnatural parity exchange ($M^\epsilon = 0^-$). In (c) is shown the 2^{++} $\omega\rho$ partial wave, while (d) shows the 4^{++} $\omega\rho$ partial wave. The curves are fits to the $\pi_1(1600)$ and $\pi_1(2015)$ (a and b), the $a_2(1700)$ in (c) and the $a_4(2040)$ in (d). (Figure reproduced from reference [69].)

In the $b_1\pi$ final state, the $\pi_1(2015)$ is produced dominantly through natural parity exchange ($M^\epsilon = 1^+$) while the $\pi_1(1600)$ was reported in both natural and unnatural parity exchange, where the unnatural exchange dominated. They observe a mass of $2.014 \pm 0.020 \pm 0.016$ GeV and a width of $0.230 \pm 0.032 \pm 0.073$ GeV which are consistent with that observed in the $f_1\pi$ final state. VES

also looked at the $b_1\pi$ final state, but did not observe 1^{-+} intensity above 1.9 GeV [72]. The reported masses and widths are summarized in Table XIV. We note that this state does not appear in the summary tables of the PDG [1].

Mode	Mass (GeV)	Width (GeV)	Experiment	Reference
$f_1\pi$	2.001 ± 0.030	0.333 ± 0.052	E852	[68]
$b_1\pi$	2.014 ± 0.020	0.230 ± 0.032	E852	[69]

TABLE XIV. Reported masses and widths of the $\pi_1(2015)$ as observed in the E852 experiment. The PDG does not report an average for this state.

With so little experimental evidence for this high-mass state, it is difficult to say much. We note that the observed decays, $f_1\pi$ and $b_1\pi$ are those expected for a hybrid meson. We also note that the production of this state is consistent (natural parity exchange) for both of the observed final states. In the case that the $\pi_1(1600)$ is associated with the lowest-mass hybrid state, one possible interpretation of the $\pi_1(2015)$ would be a excited state. The mass splitting is typical of radial excitations observed in the normal mesons. In the case of the $\pi_1(1600)$ identified as something else, the $\pi_1(2015)$ would be a prime candidate for the lightest mass hybrid.

IV. THE FUTURE

The COMPASS experiment has recently started looking at pion peripheral production similar to work carried out by both VES and E852. Two new facilities are also expected in the not-too-distant future, PANDA at GSI and GlueX at Jefferson Lab. The former will study $\bar{p}p$ annihilation in the charmonium region, but it will also be possible to search for production of light-quark hybrids. GlueX will use a 9 GeV beam of linearly polarized photons to produce hybrids.

Photoproduction of hybrids is interesting for several reasons. Simple arguments based on vector meson dominance suggest that the photon may behave like an $S = 1$ $\bar{q}q$ system. In several models, such a system is more likely to couple to exotic quantum-number hybrids. Early calculations of hybrids used the apparent large $\rho\pi$ coupling of the $\pi_1(1600)$ to suggest that this state should be produced at least as strongly as normal mesons in photoproduction [76–78]. Unfortunately, the current controversy on the $\rho\pi$ decay of the $\pi_1(1600)$ makes the underlying assumption questionable, which may be confirmed by the non observation of the $\pi_1(1600)$ by CLAS [73].

Recently, lattice calculations have been performed to compute the radiative decay of charmonium $c\bar{c}$ and hybrid states [79]. In the charmonium system, they find that there is a large radiative decay for an exotic quantum number hybrid. These studies are currently being extended to the light-quark hybrids with the goal of providing estimates of the photoproduction cross sections of

these states. However, based on the results in the charmonium sector, photoproduction appears to be a good place to look for hybrid mesons.

V. CONCLUSIONS

Over the last two decades, substantial data has been collected looking for exotic quantum-number mesons. In particular, searches have focused on hybrid mesons, which arise due to orbital excitations of the gluonic fields which confine the quarks inside the mesons. These studies have yielded evidence for three states, the $\pi_1(1400)$, the $\pi_1(1600)$ and the $\pi_1(2015)$. The $\pi_1(1400)$ has only been observed in the $\eta\pi$ decay mode. While all experiments agree that there is strength in the 1^{-+} exotic wave, there is no consensus as to the nature of the exotic wave. However, if it is indeed resonant, it most likely related to a $q\bar{q}q\bar{q}$ structure, and not a hybrid meson.

The evidence for the $\pi_1(1600)$ is the most extensive of all three states. It has been observed in four different decay modes by several experiments. While some controversy surrounds the $\rho\pi$ decay mode, and there is some confusion about how the state is produced, most people would agree that this state exists and is a good candidate for the lightest mass hybrid meson.

The evidence for the $\pi_1(2015)$ is much more limited. It has been seen by one experiment in two decay modes with very limited statistics while a second experiment (VES) does not see evidence for this state. What little is known about this state makes it a good candidate for a hybrid meson, but confirmation is clearly needed. If both the $\pi_1(1600)$ and the $\pi_1(2015)$ do exist, then the latter may be a radial excitation of the former.

To date, the crucial missing pieces of the hybrid puzzle are other members of the hybrid nonets, the η_1 and η'_1 in the case of the 1^{-+} states, and states with other exotic quantum numbers, 0^{+-} and 2^{+-} . Definitive observation of these would provide the missing information to confirm the gluonic excitations of QCD. Fortunately, there will soon be four experimental programs running (COMPASS at CERN, BES III in Beijing, PANDA at GSI and GlueX at Jefferson Lab) that can provide information on these issues.

ACKNOWLEDGMENTS

The authors would like to thank Jozef Dudek for useful discussions and comments. This work was supported in part by the U.S. Department of Energy under grant No. DE-FG02-87ER40315.

-
- [1] C. Amsler, *et al.* [The Particle Data Group], "Review of Particle Physics," *Phys. Lett. B* **667**, 1, (2008).
 - [2] T. Barnes and F. E. Close, "A Light Exotic Q Anti-Q G Hermaphrodite Meson?," *Phys. Lett. B* **116**, 365 (1982).
 - [3] Eberhard Klempt and Alexander Zaitsev, "Glueballs, Hybrids, Multiquarks Experimental Facts Versus QCD Inspired Concepts," *Phys. Rep.* **454**, 1, (2007).
 - [4] V. Crede and C. A. Meyer, "The Experimental Status of Glueballs," *Prog. Part. Nucl. Phys.* **63**, 74, (2009).
 - [5] R. L. Jaffe and K. Johnson, "Unconventional States of Confined Quarks and Gluons," *Phys. Lett. B* **60**, 201, (1976).
 - [6] A. I. Vainshtein, M. B. Voloshin, V. I. Zakharov, V. A. Novikov, L. B. Okun and M. A. Shifman, "Sum Rules For Light Quarks In Quantum Chromodynamics," *Sov. J. Nucl. Phys.* **27**, 274 (1978) [*Yad. Fiz.* **27**, 514 (1978)].
 - [7] T. Barnes, F. E. Close, F. de Viron and J. Weyers, "Q Anti-Q G Hermaphrodite Mesons In The Mit Bag Model," *Nucl. Phys. B* **224**, 241 (1983).
 - [8] M. S. Chanowitz and S. R. Sharpe, "Hybrids: Mixed States Of Quarks And Gluons," *Nucl. Phys. B* **222**, 211 (1983) [Erratum-*ibid.* **B 228**, 588 (1983)].
 - [9] I. I. Balitsky, D. Diakonov and A. V. Yung, "Exotic Mesons With $J^{PC} = 1^{-+}$ From QCD Sum Rules," *Phys. Lett. B* **112**, 71 (1982).
 - [10] J. I. Latorre, P. Pascual and S. Narison, "Spectra and hadronic couplings of light hermaphrodite mesons," *Z. Phys. C* **34**, 347, (1987).
 - [11] S. Narison, "Gluonia, scalar and hybrid mesons in QCD," *Nucl. Phys. A* **675**, 54c, (2000).
 - [12] S. Narison, "1⁻⁺ light exotic mesons in QCD," *Phys. Lett. B* **675**, 319, (2009).
 - [13] Y. Nambu, "Dual Model Of Hadrons," Univ. of Chicago report No. **70-07**, (1970).
 - [14] T. Nambu, "The Confinement of Quarks," *Sci. Am.* **235**, No.5, 48, (1976).
 - [15] G. Bali *et al.* [SESAM Collaboration], "Glueballs and string breaking from full QCD", *Nucl. Phys. Proc. Suppl.* **63**, 209, (1998).
 - [16] N. Isgur and J. Paton, "Fluxtube model for hadrons in QCD," *Phys. Rev. D* **31**, 2910, (1985).
 - [17] N. Isgur, R. Kokoski and J. Paton, "Gluonic Excitations of Mesons: Why they are missing and where to find them," *Phys Rev. Lett.* **54**, 869, (1985).
 - [18] S. R. Cotanch and F. J. Llanes-Estrada, "Relativistic many body approach to exotic and charmed hybrid mesons," *Nucl. Phys. A* **689**, (2001).
 - [19] P. Lacock *et al.*, "Hybrid mesons from quenched QCD," *Phys. Lett. B* **401**, 309, (1997).
 - [20] C. Bernard, J. E. Hetrick, T. A. Degrand, M. Wingate, C. DeTar, C. McNeile, S. Gottlieb, U. M. Heller, K. Rummulainen, B. Sugar and D. Toussaint, "Exotic mesons in quenched lattice QCD," *Phys. Rev. D* **56**, 7039, (1997).
 - [21] P. Lacock, K. Schilling [SESAM Collaboration], "Hybrid and Orbitally Excited Mesons in Full QCD," *Nucl. Phys. Proc. Suppl.* **73**, 261, (1999).
 - [22] C. Bernard *et al.*, "Exotic meson spectroscopy from the clover action at $\beta = 5.85$ and 6.15," *Nucl. Phys. B(Proc. Suppl.)* **73**, 264, (1999).
 - [23] Z. H. Mei and X. Q. Luo, "Exotic mesons from quantum chromodynamics with improved gluon and quark actions

- on the anisotropic lattice,” *Int. J. Mod. Phys. A* **18**, 5713 (2003).
- [24] C. Bernard, T. Burch, C. DeTar, Steven Gottlieb, E.B. Gregory, U.M. Heller, J. Osborn, R. Sugar and D. Toussaint, “Lattice calculation of 1^{-+} hybrid mesons with improved Kogut-Susskind fermions,” *Phys. Rev. D* **68**, 074505, (2003).
- [25] J. N. Hedditch *et al.*, “ 1^{-+} exotic meson at light quark masses,” *Phys. Rev. D* **72**, 114507, (2005).
- [26] C. McNeile and C. Michael [UKQCD Collaboration], “Decay width of light quark hybrid meson from the lattice,” *Phys. Rev. D* **73**, 074506 (2006).
- [27] J. J. Dudek *et al.* [Hadron Spectrum Collaboration], “Highly excited and exotic meson spectrum from dynamical lattice QCD,” *Phys. Rev. Lett.* **102**, 262001, (2009).
- [28] Jozef J. Dudek, Robert G. Edwards, Michael J. Peardon, David G. Richards, Christopher E. Thomas, “Toward the excited meson spectrum of dynamical QCD,” arXiv:1004930 [hep-lat], (2010).
- [29] Jozef Dudek, private communication.
- [30] E. S. Ackleh, T. Barnes and E. S. Swanson, “On the mechanism of open flavor strong decays,” *Phys. Rev. D* **54**, 6811, (1996).
- [31] T. Barnes, F. E. Close, P. R. Page and E. S. Swanson, “Higher quarkonia,” *Phys. Rev. D* **55**, 4157, (1997).
- [32] F. E. Close and P. R. Page, “The production and decay of hybrid mesons by flux-tube breaking,” *Nucl. Phys. B* **443**, 23, (1995).
- [33] P. R. Page, E. S. Swanson and A. P. Szczepaniak, “Hybrid Meson Decay Phenomenology,” *Phys. Rev. D* **59**, 034016 (1999).
- [34] F. E. Close and C. E. Thomas, “Looking for a gift of Nature: Hadron loops and hybrid mixing,” *Phys. Rev. C* **79**, 045201 (2009).
- [35] T. Barnes and E. S. Swanson, “Hadron Loops: General Theorems and Application to Charmonium,” *Phys. Rev. C* **77**, 055206 (2008).
- [36] P. R. Page, “Why hybrid meson coupling to two S wave mesons is suppressed,” *Phys. Lett. B* **402**, 183 (1997).
- [37] F. E. Close and J. J. Dudek, “The ‘forbidden’ decays of hybrid mesons to $\pi\rho$ can be large,” *Phys. Rev. D* **70**, 094015 (2004).
- [38] C. McNeile and C. Michael, “Hybrid meson decay from the lattice,” *Phys. Rev. D* **65**, 094505, (2002).
- [39] T. J. Burns and F. E. Close, “Hybrid-meson properties in lattice QCD and flux-tube models,” *Phys. Rev. D* **74**, 034003, (2006).
- [40] S. U. Chung, E. Klempt and J. G. Korner, “SU(3) classification of p-wave eta pi and eta’ pi systems,” *Eur. Phys. J. A* **15**, 539 (2002).
- [41] C. J. Morningstar and M. J. Peardon, “The glueball spectrum from an anisotropic lattice study,” *Phys. Rev. D* **60**, 034509 (1999).
- [42] R. L. Jaffe and F. E. Low, “The connection between quark-model eigenstates and low-energy scattering,” *Phys. Rev. D* **19**, 2105, (1979).
- [43] S. U. Chung and T. L. Trueman, “Positivity Conditions On The Spin Density Matrix: A Simple Parametrization,” *Phys. Rev. D* **11**, 633 (1975).
- [44] S. U. Chung *et al.*, “Evidence for exotic J(PC) = 1-+ meson production in the reaction $\pi^- p \rightarrow \eta\pi^- p$ at 18-GeV/c,” *Phys. Rev. D* **60**, 092001, (1999).
- [45] A. Binosi and L. Theussl, “JaxoDraw: A graphical user interface for drawing Feynman diagrams,” *Comp. Phys. Comm.* **161**, 76 (2004).
- [46] D. Alde *et al.*, “Evidence for a 1^{-+} Exotic Meson,” *Phys. Lett. B* **205**, 397, (1988).
- [47] W. D. Apel *et al.*, “Analysis Of The Reaction $\pi^- p \rightarrow \pi^0\eta n$ At 40-GeV/C Beam Momentum,” *Nucl. Phys. B* **193**, 269, (1981).
- [48] H. Aoyagi *et al.*, “Study of the $\eta\pi^-$ system in the $\pi^- p$ reaction at 6.3-GeV/c,” *Phys. Lett. B* **314**, 246, (1993).
- [49] G. M. Beladidze *et al.* [VES Collaboration], “Study of $\pi^- N \rightarrow \eta\pi^- N$ and $\pi^- N \rightarrow \eta'\pi^- N$ reactions at 37 GeV/c,” *Phys. Lett. B* **313**, 276, (1993).
- [50] V. Dorofeev, *et al.* [VES Collaboration], “The $J^{PC} = 1^{-+}$ hunting season at VES,” *AIP Conf. Proc.* **619**, 143, (2002).
- [51] D. V. Amelin *et al.* [VES Collaboration], “Investigation of hybrid states in the VES experiment at the Institute for High Energy Physics (Protvino),” *Phys. At. Nucl.* **68**, 359, (2005).
- [52] D. R. Thompson *et al.* [E852 Collaboration], “Evidence for exotic meson production in the reaction $\pi^- p \rightarrow \eta\pi^- p$ at 18-GeV/c,” *Phys. Rev. Lett.* **79**, 1630 (1997).
- [53] A. Abele *et al.* [The Crystal Barrel Collaboration], “Exotic $\eta\pi$ state in $\bar{p}d$ annihilation at rest into $\pi^-\pi^0\eta p$ (spectator),” *Phys. Lett. B* **423**, 175 (1998).
- [54] A. Abele *et al.* [The Crystal Barrel Collaboration], “Evidence for a $\pi\eta$ P wave in $\bar{p}p$ annihilations at rest into $\pi^0\pi^0\eta$,” *Phys. Lett. B* **446**, 349 (1999).
- [55] A. R. Dzierba *et al.*, “Study of the $\eta\pi^0$ spectrum and search for a $J^{PC} = 1^{-+}$ exotic meson,” *Phys. Rev. D* **67**, 1, (2003).
- [56] G. S. Adams *et al.* [E852 Collaboration], “Confirmation of a π_1^0 Exotic Meson in the $\eta\pi^0$ System,” *Phys. Lett. B* **657**, 27 (2007).
- [57] P. Salvini *et al.* [Obelix Collaboration], “ $\bar{p}p$ annihilations into four charged pions in flight and at rest,” *Eur. Phys. J. C* **35**, 21, (2004).
- [58] W. Duenweber and F. Meyer-Wildhagen, “Exotic states in Crystal Barrel analyses of annihilation channels,” *AIP Conf. Proc.* **717**, 388, (2004).
- [59] A. Donnachie and P. R. Page, “Interpretation of Experimental J(PC) Exotic Signals,” *Phys. Rev. D* **58**, 114012 (1998).
- [60] A. P. Szczepaniak, M. Swat, A. R. Dzierba and S. Teige, “Study of the $\eta\pi$ and $\eta'\pi$ spectra and interpretation of possible exotic $J^{PC} = 1^{-+}$ mesons,” *Phys. Rev. Lett.* **91**, 092002 (2003).
- [61] Yu. P. Gouz *et al.* [VES Collaboration], “Study of the wave with $J^{PC} = 1^{-+}$ in the partial wave analysis of $\eta'\pi^-$, $\eta\pi^-$, $f_1\pi^-$ and $\rho^0\pi^-$ systems produced in $\pi^- N$ interactions at $p_\pi = 37$ GeV/c,” *AIP Conf. Proc.* **272**, 572 (1993).
- [62] G. S. Adams *et al.* [E852 Collaboration], “Observation of a new $J^{PC} = 1^{-+}$ exotic state in the reaction $\pi^- p \rightarrow \pi^+\pi^-\pi^- p$ at 18-GeV/c,” *Phys. Rev. Lett.* **81**, 5760 (1998).
- [63] S. U. Chung *et al.* [E852 Collaboration], “Exotic and $q\bar{q}$ resonances in the $\pi^+\pi^-\pi^-$ system produced in $\pi^- p$ collisions at 18 GeV/c,” *Phys. Rev. D* **65**, 072001, (2002).
- [64] Yu A. Khokholov, *et al.* [VES Collaboration], “Study of $X(1600)1^{-+}$ hybrid,” *Nucl. Phys. A* **663**, 596, (2000).
- [65] A. Zaitsev, *et al.* [VES Collaboration], “Study of exotic resonances in diffractive reactions,” *Nucl. Phys. A* **675**, 155c, (2000).
- [66] E. I. Ivanov *et al.* [E852 Collaboration], “Observation of

- exotic meson production in the reaction $\pi^- p \rightarrow \eta' \pi^- p$ at 18 GeV/c,” Phys. Rev. Lett. **86**, 3977 (2001).
- [67] C. A. Baker *et al.*, “Confirmation of $a_0(1450)$ and $\pi_1(1600)$ in $\bar{p}p \rightarrow \omega\pi^+\pi^-\pi^0$ at rest,” Phys. Lett. B **563**, 140 (2003).
- [68] J. Kuhn *et al.* [E852 Collaboration], “Exotic meson production in the $f_1(1285)\pi^-$ system observed in the reaction $\pi^- p \rightarrow \eta\pi^+\pi^-\pi^- p$ at 18 GeV/c,” Phys. Lett. B **595**, 109 (2004).
- [69] M. Lu *et al.* [E852 Collaboration], “Exotic meson decay to $\omega\pi^0\pi^-$,” Phys. Rev. Lett. **94**, 032002 (2005).
- [70] V. Dorofeev [VES Collaboration], “New results from VES,” arXiv:hep-ex/9905002 (1999).
- [71] A. R. Dzierba *et al.*, “A partial wave analysis of the $\pi^-\pi^-\pi^+$ and $\pi^-\pi^0\pi^0$ systems and the search for a $J^{PC} = 1^{-+}$ meson,” Phys. Rev. D **73**, 072001 (2006).
- [72] D. V. Amelin *et al.*, “Investigation of hybrid states in the VES experiment at the Institute for High Energy Physics (Protvino),” Phys. Atom. Nucl. **68**, 359 (2005) [Yad. Fiz. **68**, 388 (2005)].
- [73] M. Nozar *et al.* [CLAS Collaboration], “Search for the photo-excitation of exotic mesons in the $\pi^+\pi^+\pi^-$ system,” Phys. Rev. Lett. **102**, 102002, (2009).
- [74] A. Alekseev *et al.* [The COMPASS Collaboration], “Observation of a $J^{PC} = 1^{-+}$ exotic resonance in diffractive dissociation of 190 GeV/c π^- into $\pi^-\pi^-\pi^+$,” arXiv:0910.5842 [hep-ex] (2009).
- [75] B. Grube *et al.* [The COMPASS Collaboration], “Precision Meson Spectroscopy at COMPASS,” arXiv:1002.1272 [hep-ex] (2010).
- [76] A. V. Afansev and A. P. Szczepaniak, “Charge exchange $\rho^0\pi^+$ photoproduction and implications for searches of exotic meson,” Phys. Rev. D **61**, 114008, (2000).
- [77] A. P. Szczepaniak and M. Swat, “Role of Photoproduction in Exotic Meson Searches,” Phys. Lett. B **516**, 72 (2001).
- [78] F. E. Close and J. J. Dudek, “The ”forbidden” decays of hybrid mesons to $\pi\rho$ can be large,” Phys. Rev. D **70**, 094015, (2003).
- [79] J. J. Dudek, R. Edwards and C. E. Thomas, “Exotic and excited-state radiative transitions in charmonium from lattice QCD,” Phys. Rev. D **79**, 094504 (2009).